General Disclaimer

One or more of the Following Statements may affect this Document

- This document has been reproduced from the best copy furnished by the organizational source. It is being released in the interest of making available as much information as possible.

- This document may contain data, which exceeds the sheet parameters. It was furnished in this condition by the organizational source and is the best copy available.

- This document may contain tone-on-tone or color graphs, charts and/or pictures, which have been reproduced in black and white.

- This document is paginated as submitted by the original source.

- Portions of this document are not fully legible due to the historical nature of some of the material. However, it is the best reproduction available from the original submission.

(NASA-CR-174809) ADVANCED GAS TURBINE (AGT) POWERTRAIN SYSTEM DEVELOPMENT FOR AUTOMOTIVE APPLICATIONS Semiannual Progress Report, Jul. - Dec. 1983 (Garrett Turbine Engine Co.) 70 p HC A04/MF A01 CSCL 13F G3/85 N85-18831 Unclas 14124

DOE/NASA/0167-8
NASA CR-174809
GARRETT NO. 31-3725(8)

ADVANCED GAS TURBINE (AGT) TECHNOLOGY DEVELOPMENT

EIGHTH SEMIANNUAL PROGRESS REPORT
(JULY 1983 — DECEMBER 1983)

Engineering Staff of
Garrett Turbine Engine Company
A Division of The Garrett Corporation

JUNE 1984

Prepared for
NATIONAL AERONAUTICS AND SPACE ADMINISTRATION
Lewis Research Center
Cleveland, Ohio 44135
Under Contract DEN3-167

for

U.S. DEPARTMENT OF ENERGY
Office of Vehicle and Engine Research and Development
Technology Development and Analysis Division
Washington D.C. 20585

DOE/NASA/0167-8
NASA CR-174809
GARRETT NO. 31-3725(8)

ADVANCED GAS TURBINE (AGT) TECHNOLOGY DEVELOPMENT

EIGHTH SEMIANNUAL PROGRESS REPORT
(JULY 1983 — DECEMBER 1983)

Engineering Staff of
Garrett Turbine Engine Company
A Division of The Garrett Corporation

JUNE 1984

Prepared for
NATIONAL AERONAUTICS AND SPACE ADMINISTRATION
Lewis Research Center
Cleveland, Ohio 44135
Under Contract DEN3-167

for

U.S. DEPARTMENT OF ENERGY
Office of Vehicle and Engine Research and Development
Technology Development and Analysis Division
Washington D.C. 20585

TABLE OF CONTENTS

TABLE OF CONTENTS (Contd)

TABLE OF CONTENTS (Contd)

LIST OF FIGURES

LIST OF FIGURES (Contd)

LIST OF TABLES

1.0 SUMMARY

This report describes progress and work performed by the Garrett/Ford team to develop an Advanced Gas Turbine (AGT) engines for automotive applications, during the period July through December 1983. This work was performed for the Department of Energy under NASA Contract DEN3-167. This is the eighth in a series of semi-annual reports. Work performed during the first seven periods (References 1 through 7) initiated design and analysis, ceramic development component testing, and test bed evaluation.

Project effort conducted under this contract is part of the DOE* Gas Turbine Highway Vehicle System Program. This program is oriented at providing the United States automotive industry the high-risk long-range technology necessary to produce gas turbine engines for automobiles with reduced fuel consumption and reduced environmental impact. It is intended that technology resulting from this program reach the marketplace by the early 1990s.

The advanced automotive gas turbine, when installed in a Ford vehicle (3000 pounds inertia weight), will provide:

- A CFDC fuel economy of 42.8 miles per gallon based on Environmental Protection Agency (EPA) test procedures and Diesel No. 2 fuel. The AGT-powered vehicle will substantially give the same overall vehicle driveability and performance as a comparable production vehicle powered by a conventional spark-ignition powertrain system
- Emissions less than federal standards
- Ability to use a variety of fuels

*A list of abbreviations and acronyms is presented in Appendix D, herein.

1.1 Power Section Development

Rotor dynamic instability investigations continued on engines S/N 001 and 003. Several forward ball bearing hydraulic mount configurations were tested with little effect. Foil bearing parameters such as stiffness, foil number, load capacity and sway space were changed with some benefits noted. Initial investigations into aerodynamic influences were evaluated and a shaft damper system was tested with marginal results.

Trial assembly of S/N 002 ceramic engine was initiated and testing plans and procedures established.

1.2 Compressor Development

Impeller design activities have been completed on the straight line element (SLE) blade definition to address near-net-shape powder metal die forging. Performance characteristics of the Baseline Test 2A impeller were closely preserved. Duplication of the Test 2A impeller exit blade angle could not be fully accommodated using SLE methodology (50.71 degree baseline, 47.97 degree SLE). This lower exit blade angle gives rise to a lower slip factor and slightly higher work for the same tip diameter. Therefore, tip radius was reduced 0.016 inch to compensate for the reduction in average exit blade angle. All other salient design features were satisfactorily preserved.

1.3 Turbine Development

The modified blading design has been released to the subcontractors for tooling procurement. No other activity was addressed during this reporting period.

1.4 Combustor Development

Developmental testing of the diffusion flame combustor (DFC) for initial use in the

S/N 002 2100°F ceramic structures engine was completed. Combustor wall temperatures were recorded at idle and maximum power conditions, and the combustor pattern factor was within acceptable limits.

A natural gas slave preheater was designed and fabricated, while the nonvitiated preheater was repaired.

A film cooled version of the Delavan simplex nozzle was received and is being readied for test.

1.5 Regenerator Development

Samples of a new rectangular matrix (1100 cell/in^2) were received from NGK, along with the first full size core. Modulus of rupture (MOR) is equivalent to the original thick wall isosceles triangular structure. In addition, three Corning thinwall sinusoidal wrapped cores also were received.

Hot regenerator rig testing of the Phase IV seal was accomplished. The main objective of the Phase IV design was to maintain the leakage characteristics of the Phase III while reducing the drive torque requirements. Three different combinations of the Phase IV seal design were evaluated. The best of these then was selected for evaluation at various build clearances to determine the effect of diaphragm clearance on leakage and drive torque.

Based on test data from Phase IV, initial fabrication of Phase V seals was accomplished. Preliminary static seal rig testing showed a significant reduction in leakage and sensitivity to stack height. In addition, the drive torque requirements were reduced. Seals currently are being made available for hot regenerator rig testing.

1.6 Ceramic Development

Ceramic screening tests were completed qualifying components for structures rig testing at 2000°F. Two complete sets of ceramic static structures were qualified for engine testing. The components successfully passed a minimum of 7 simulated engine startup and shutdown transients to 2000°F. A total of 13 hours and 31 minutes were accumulated during this reporting period in the structures rig.

Seven rotors fabricated by ACC (8-percent Y_2O_2, 4-percent Al_2O_3) were sintered during this reporting period (four by Ford and three by ACC). Three rotors have passed NDE inspection and are being machined for spin testing. Two rotors were sectioned for test bar evaluation with results indicating 113 ksi at room temperature and 54 ksi at 2200°F. Three rotors were delivered to ASEA-Sweden for glass encapsulation and HIP experiments. Densities ranged from 95-99 percent theoretical. Although these rotors were not considered good quality (visual, bladefill, etc) one rotor was selected for spin test.

1.7 Rotor Dynamics/Foil Bearing Development

Effort continued on rotor dynamics development in support of resolving the subsynchronous motion noted during engine testing. Activities have included screening foil bearings for engine test, evaluation of a shaft damper, and initiating a thorough thermal mapping of the test rig and engine bearing environment. In addition, alternate bearing configurations are being investigated on an active basis.

2.0 INTRODUCTION

This report is the eighth in a series of Semi-annual Technical Summary Reports for the Advanced Gas Turbine (AGT) Technology Development Project, authorized under NASA Contract DEN3-167 and sponsored by the Department of Energy (DOE). This report has been prepared by The Garrett Turbine Engine Company (hereinafter referred to as Garrett), a Division of The Garrett Corporation, and includes information provided by Ford Motor Company, the Carborundum Company, and AiResearch Casting Company. The project is administered by Mr. Roger Palmer, Project Manager, NASA-Lewis Research Center, Cleveland, Ohio. This report presents plans and progress from July 1983 through December 1983.

Project effort conducted under this contract is part of the DOE Gas Turbine Highway Vehicle System Program. This program is oriented at providing the United States automotive industry the high risk, long range technology necessary to produce gas turbine engines for automobiles that will have reduced fuel consumption and reduced environmental impact. It is intended that technology resulting from this program be capable of reaching the marketplace by the early 1990s.

The advanced automotive gas turbine, when installed in a Ford vehicle (3000 pounds inertia weight) would provide:

- A CFDC fuel economy of 42.8 miles per gallon based on Environmental Protection Agency (EPA) test procedures and Diesel No. 2 fuel. The AGT-powered vehicle shall give substantially the same overall vehicle driveability and performance as a comparable production vehicle powered by a conventional spark-ignition powertrain system
- Emissions less than federal standards
- Ability to use variety of fuels

The Garrett/Ford Advanced Automotive Gas Turbine has been designated the AGT101.

The program is oriented toward developing the long range high risk technology of the AGT101 gas turbine such that the auto industry can carry that technology forward to production in the 1990s. Emphasis on ceramics, gas bearings, low emission combustion and improved component performance dominates the effort. The AGT101 gas turbine is being used as a test bed in which to develop these technologies.

The program, as currently scheduled, is depicted in Figure 1. The program continues techology work through FY85, culminating in the demonstration of the original goals of engine specific fuel consumption, power output, and emissions. In addition, the viability of ceramics will have been demonstrated in the AGT101 test beds, and the potential of economically producing the ceramic parts in automotive production quantities will have been assessed. When these goals are achieved, Ford will be in a position to initiate the production process without Government support, through the typical preproduction task, which then could lead to production in the 1990s.

The primary technology challenge in the program continues to be the development of the ceramic components and related high performance gas turbine aerothermodynamic components for the AGT101. The AGT101 is nominally a 100 shp engine, capable of speeds to 100,000 rpm and operating at turbine inlet temperatures (TIT) to 2500°F with a specific fuel consumption level of 0.3 over much of the operating range.

This report reviews the power section (metal and ceramic engine) effort conducted to date, followed by a review of the component/ceramic technology development. Appendices include reports of progress from Ford, AiResearch Casting Company, and the Carborundum Company.

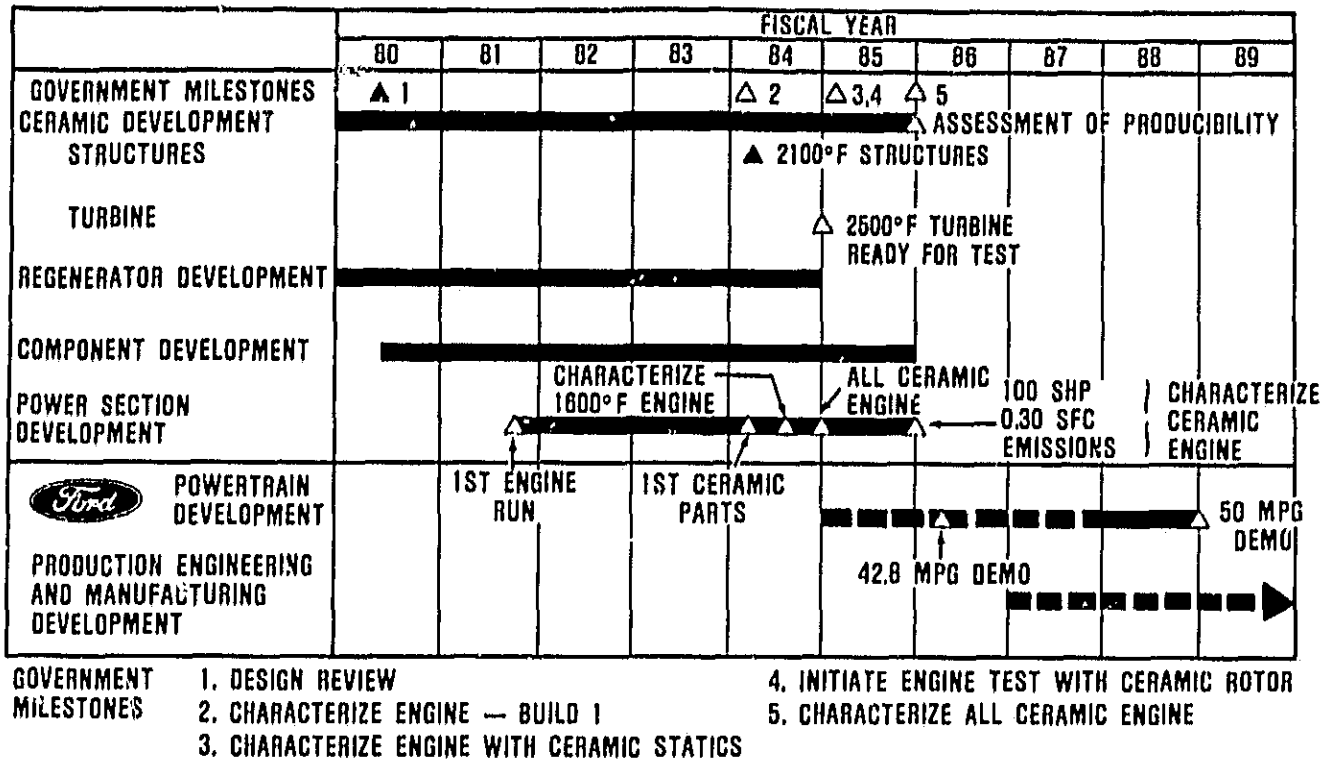

Figure 1. AGT101 Program Schedule.

3.0 POWER SECTION DEVELOPMENT

Rotor dynamic instability testing continued on engine S/Ns 001 and 003. Several forward ball bearing hydraulic mount configurations were tested with little effect. Changes were made in the foil bearing parameters such as stiffness, load capacity, foil number, and sway space with some benefits noted. Aerodynamic influences were investigated along with a shaft damper system.

Trial assembly of S/N 002 ceramic engine was initiated and plans prepared for initial testing during the next reporting period.

3.1 Rotor Dynamic Development

Rotor dynamic development to increase stability continued through this reporting period. This effort has included changes to the forward ball bearing mounting, increasing foil bearing stiffness by changing foil thickness, foil number and bearing sway space; and by adding shaft dampers. In addition, some diagnostic testing was conducted to determine possible sources of dynamic excitation. Engine S/N 003, the primary rotor dynamics test bed, was tested 22 times and accumulated 8.7 hours run time and 67 starts. Engine S/N 001 was tested seven times and accumulated 7.2 hours run time and 11 starts. Some of these tests were terminated because of synchronous motion. However, during most of the tests the rotating group exhibited a subsynchronous conical motion. This motion, depicted in Figure 2, has not damaged engine hardware, except for occasional foil bearing distress, but the relatively large amplitudes (1-4 mil motion at the turbine end) have limited engine speed between 58,000 and 96,000 rpm depending on test configuration. The subsynchronous motion is a forward whirl with a frequency range of 55 to 105-Hertz, which approximates the first critical frequency. This conical motion has its maximum displacement at the turbine end with the node occurring at the ball bearing.

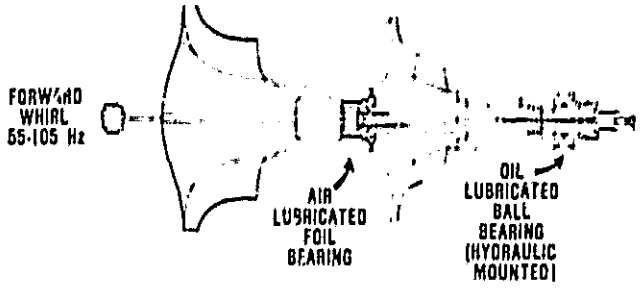

Figure 2. Rotor Exhibits Subsynchronous Conical Motion Which Limits Engine Speed.

The foil bearing stiffness was increased from 1000 to 5500 pounds/inch by changing the foil number from 7 to 6 and the foil thickness from 0.006 to 0.007 inches. The initial test of this configuration attained a speed of 96,000 rpm; however, subsequent builds deteriorated in dynamic stability.

To increase rotor damping, Engine S/N 001 was configured with three different hydraulic mount configurations for the forward ball bearing. Testing of these configurations showed little promise compared to the baseline engine. (Table 1).

A major change was made in the foil bearing by installing a relatively low stiffness (1500 pounds/inch at 0.006 inch sway space*) bearing with very high load capacity. The load capacity was measured to be 57 pounds compared to 10 pounds for the 5500 pounds/inch bearing.

The first test with this configuration achieved a speed of 76,000 rpm, a 25-percent increase from the previous test with the low load capacity bearing.

Aerodynamic clearances were tested in two of the five areas shown in Figure 3.

*Diametral clearance, bearing ID (minus) shaft OD.

TABLE 1. S/N 001 ROTOR DYNAMIC SUMMARY.

Build	10	11	12	13	14	15	16
Thrust Bearing	Hydraulic Mount Standard	Compound Parallel Mount (dry)	Button Elastomer Mount (dry)	Ring Elastomer Mount	Compound Parallel Standard	Hydraulic Mount Standard	Hydraulic Mount Standard
Foil Bearing	6 foil springless 0.0088 S.S.	6 foil springless 0.0088 S.S.	6 foil springless 0.0088 S.S.	6 foil springless 0.0088 S.S.	6 foil springless 0.0088 S.S.	7 foil L.A. type 0.006 S.S.	7 foil L.A. type 0.006 S.S.
Gearbox	Quill	Quill	Quill	Quill	Close Coupled	Quill	Quill
Max Speed (krpm)	71.0 (Unloaded	66 (Unloaded)	70.5 (Unloaded)	68.6 (Unloaded)	70.2 (Unloaded 75.5 (Loaded)	54.7 (Unloaded)	58 (Unloaded)
Vibration at Shut Down	1.3 at 96 Hz	1.4 at 100 Hz	1.4 at 100 Hz	1.5 at 104 Hz	1.24 at 105 Hz (Unloaded) 0.3 at 108 (Loaded)	1.2 at 76	3.5 at 88

The bearing housing clearance (clearance 3 in Figure 3) was increased from 0.0085 inch cylindrical to 0.0145 grooved as shown in Figure 4. This clearance was later increased to 0.040 inch cylindrical. No significant dynamic effect was noted due to changes in this clearance.

The compressor backface clearance (number 4 in Figure 3) also was changed to determine its effect on rotor dynamics. This clearance was changed from 0.024 to 0.054 and 0.079 inch clearance. The instability whirl frequency increased with each increase in clearance. The relationship is plotted in Figure 5. With the 0.079 inch clearance the engine was run to 85,000 rpm. There is an apparent inconsistency between the significant increase in frequency without a corresponding increase in stability. This inconsistency will be investigated.

A brush seal used in some gas turbine engine applications to replace a labyrinth seal was manufactured to a size that could be installed next to the foil bearing (see Figure 6). The brush seal was configured to interfere with the shaft by 0.020 inch (diametral). This would increase the frictional forces and inherent damping without adding significant stiffness or excessive power loss to the system.

The introduction of the brush seal was coupled with decreasing the sway space in the foil bearing. The foil bearing was tested at 0.0084 inch sway space as a baseline prior to adding the brush seal. Engine speed was increased from 62,000 rpm to 84,000-94,000 rpm by adding the brush seal. Sway space was decreased to 0.0064 inch and finally to 0.0034 inch with the brush seal. No additional benefits were noted by decreasing the sway space. Whether the improvements in stability with the brush seal were due to added damping or the thermal reduction of sway space in the foil bearing through additional heat generation

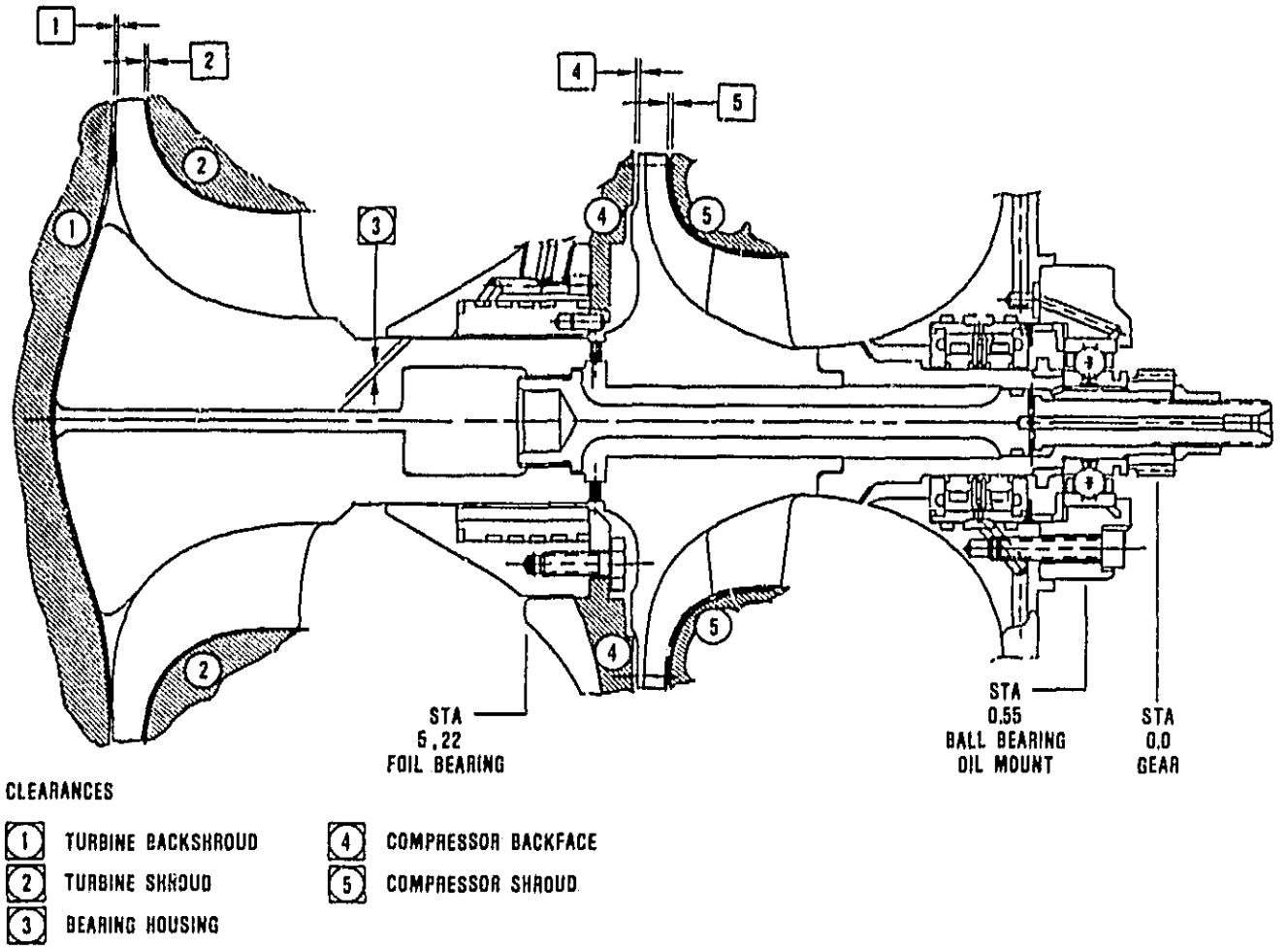

Figure 3. Rotor/Bearing System Clearances.

by the brush seal adjacent to the foil bearing is not clear. However, the brush seal has exhibited significant wear during test which would diminish its effect with time, and thus, it appears, that a brush seal is not a viable solution for stabilizing the rotor/bearing system.

Planned development in rotor dynamics for the next reporting period includes; experimentally mapping the thermal environment of the foil bearing, completing the investigation of clearance effects, adding damping with structural dampers and a hydrodynamic thrust bearing.

3.2 Ceramic Engine Development

Trial build preparations for the first 2100°F engine containing a full compliment of ceramic structures, was completed in October 1983.

Two trial assemblies of the S/N 002 ceramic engine were completed and a total engine leak check was made to establish the estimated self-sustaining temperature of the unit (Figure 7). The analysis accounted for the measured static leakage, rotor clearance effects and the hydraulic loader parasitic drag as a function of engine speed.

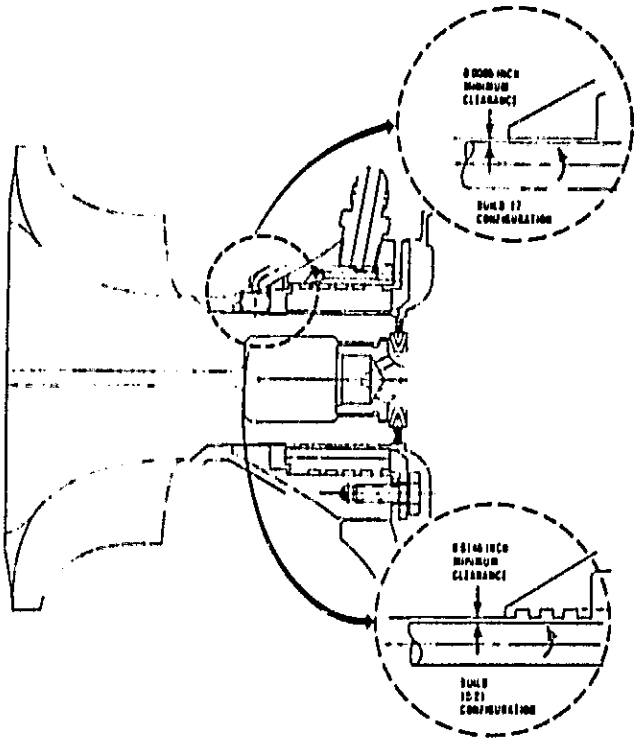

Figure 4. Configuration Differences.

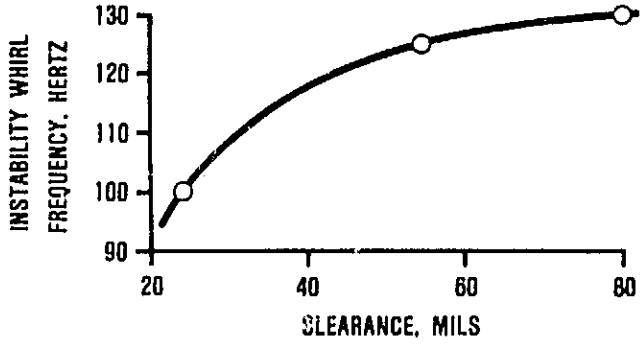

Figure 5. Compressor Backshroud Clearance Effect.

The primary purpose of the Build 1 test is to subject the first AGT101 ceramic engine configuration to a thermal cycle limited to 2100°F TIT and 65,000 rpm rotor speed. The engine will be operated along a controlled closed-loop turbine inlet temperature schedule.

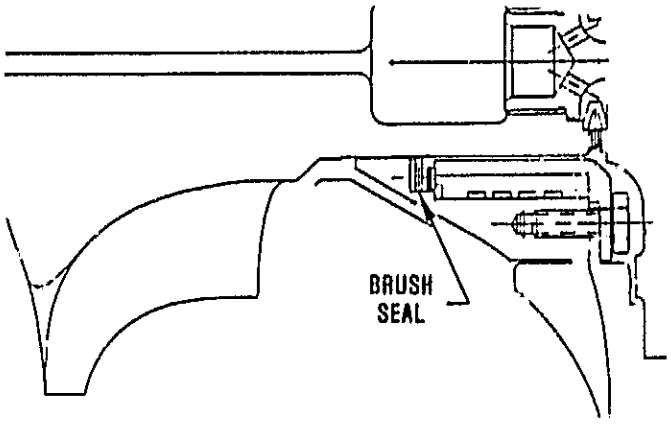

Figure 6. Brush Seal Installation.

Figure 8 gives a description of the start transient showing engine light-off to 1000°F (on the starter) and maintaining that temperature for ten minutes at idle speed, then ramping temperature up to 2100°F (approximately 42 to 43°F/minute). At approximately 1750°F, estimated engine self-sustaining temperature at idle speed, the starter assist will be removed, and the engine will be loaded to achieve a 2100°F TIT. This temperature will be maintained for three minutes prior to reducing the engine load, and thereby decreasing TIT along an identical downward ramp until all load is removed. Fuel flow will be reduced to further drop TIT. At a minimum speed of 45,000 rpm, the engine will be shut down.

With the completion of the two trial builds, engine leak check, and analysis, the final build and testing will be initiated during the next reporting period.

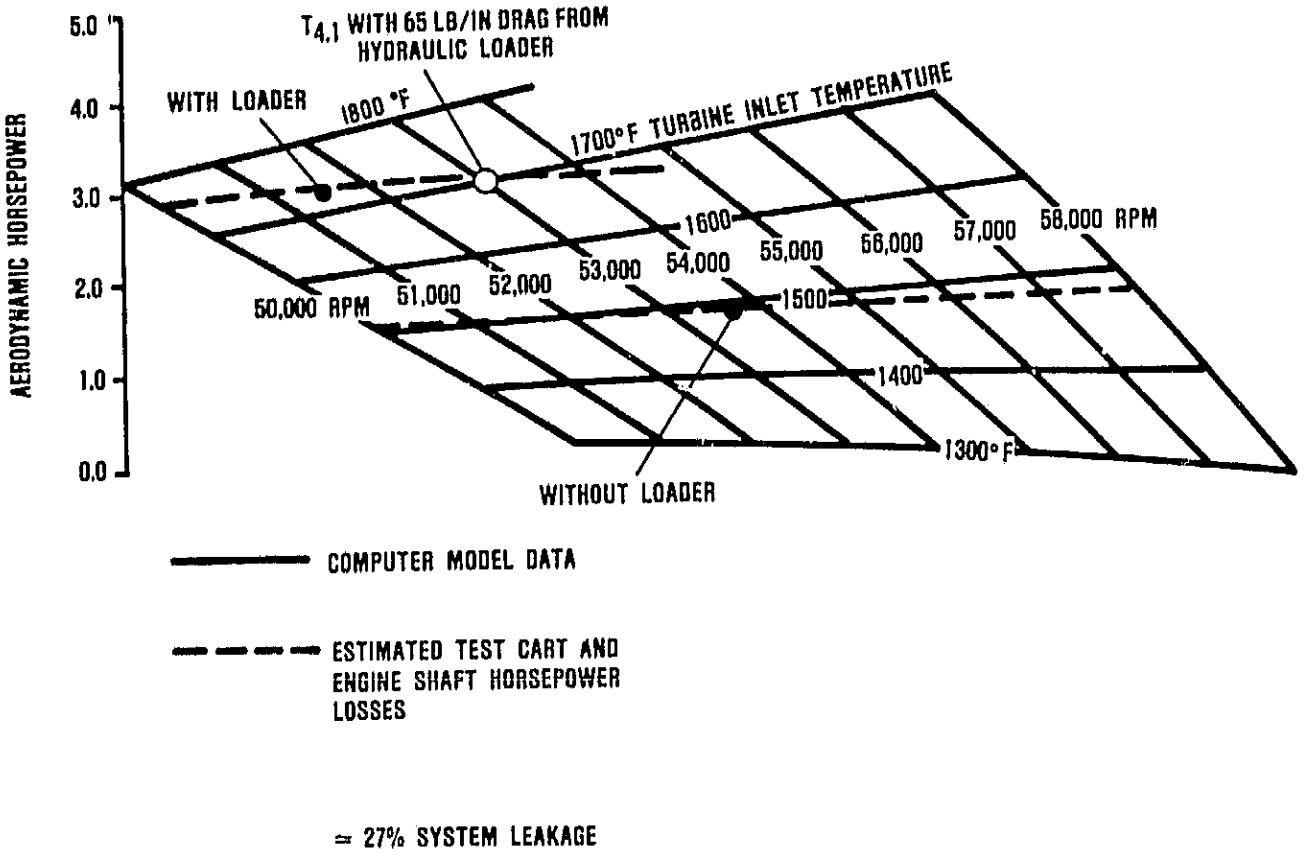

Figure 7. Engine Self-Sustaining Temperature and Speed Prediction.

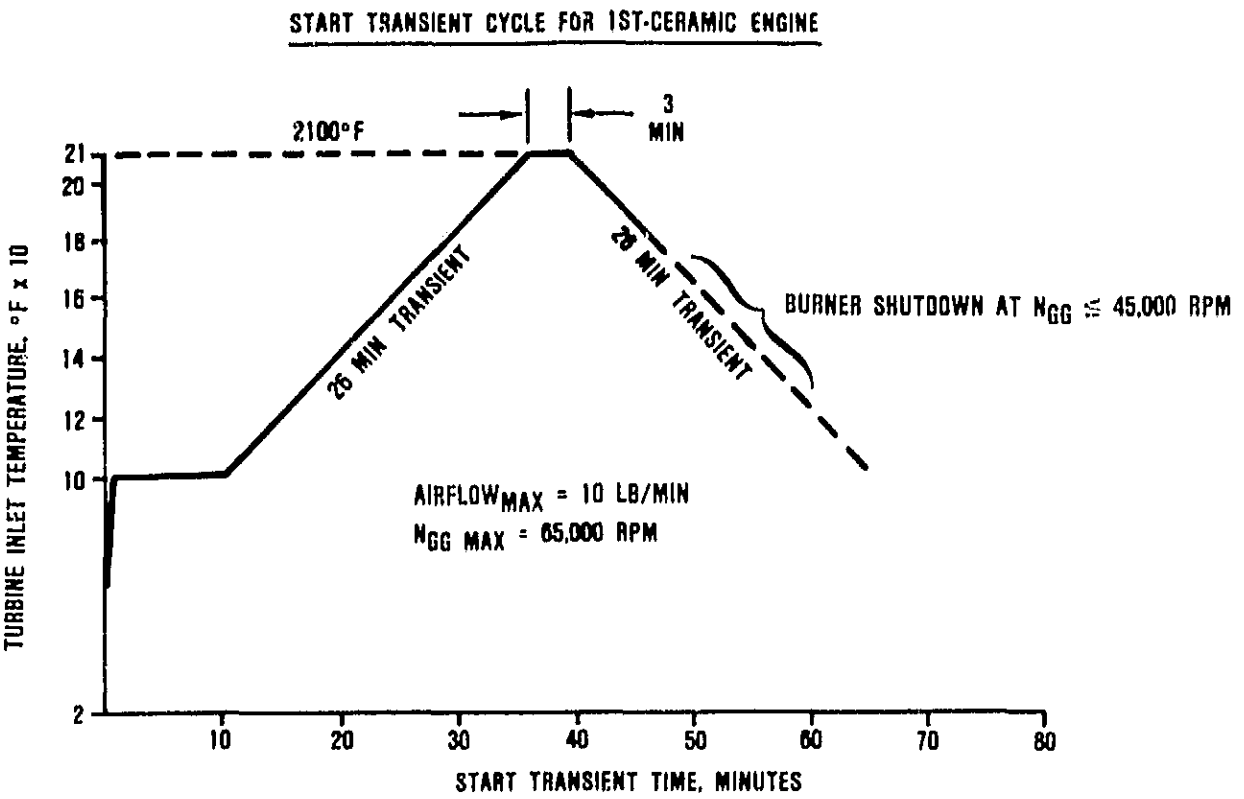

Figure 8. Start Transient Cycle for First Ceramic Engine Build S/N 002C.

4.0 COMPONENT/SUBSYSTEM DEVELOPMENT

Component/subsystem development activities during this reporting period were concentrated on supporting AGT101 (1600°F and 2100°F) engine development, ceramic development, combustion tests and hot regenerator testing. Figure 9 shows the performance rating stations for the AGT101 engine and components.

The following sections discuss major efforts and accomplishments during this reporting period for each component/subsystem.

4.1 Compressor

Impeller redesign activities have been completed on the straight line element (SLE) blade definition to address near-net-shape powder metal die forging. The basis of the redesign was to maintain the performance level demonstrated during Test 2A (Reference 6) while approximating the arbitrary blade shape using straight line elements. Table 2 shows a geometric comparison of the Test 2A impeller and the SLE impeller, while

1.0 AMBIENT
2.0 COMPRESOR INLET (IGV)
2.05 IMPELLER INLET
2.5 DIFFUSER INLET
3.0 DIFFUSER DISCHARGE
3.05 DUCT COMMON INSTRUMENTATION PLANE (RIGS)
3.1 REGENERATOR HP INLET
3.5 REGENERATOR HP EXIT
3.6 COMBUSTOR INLET
4.0 COMBUSTOR EXIT, TURBINE INLET
4.1 STATOR INLET
4.5 STATOR DISCHARGE
5.0 TURBINE ROTOR EXIT
5.05 DIFFUSER EXIT (RIGS)
5.07 DIFFUSER EXIT BEND (RIGS)
5.1 REGENERATOR LP INLET
5.5 REGENERATOR LP EXIT
7.0 POWER SECTION EXHAUST

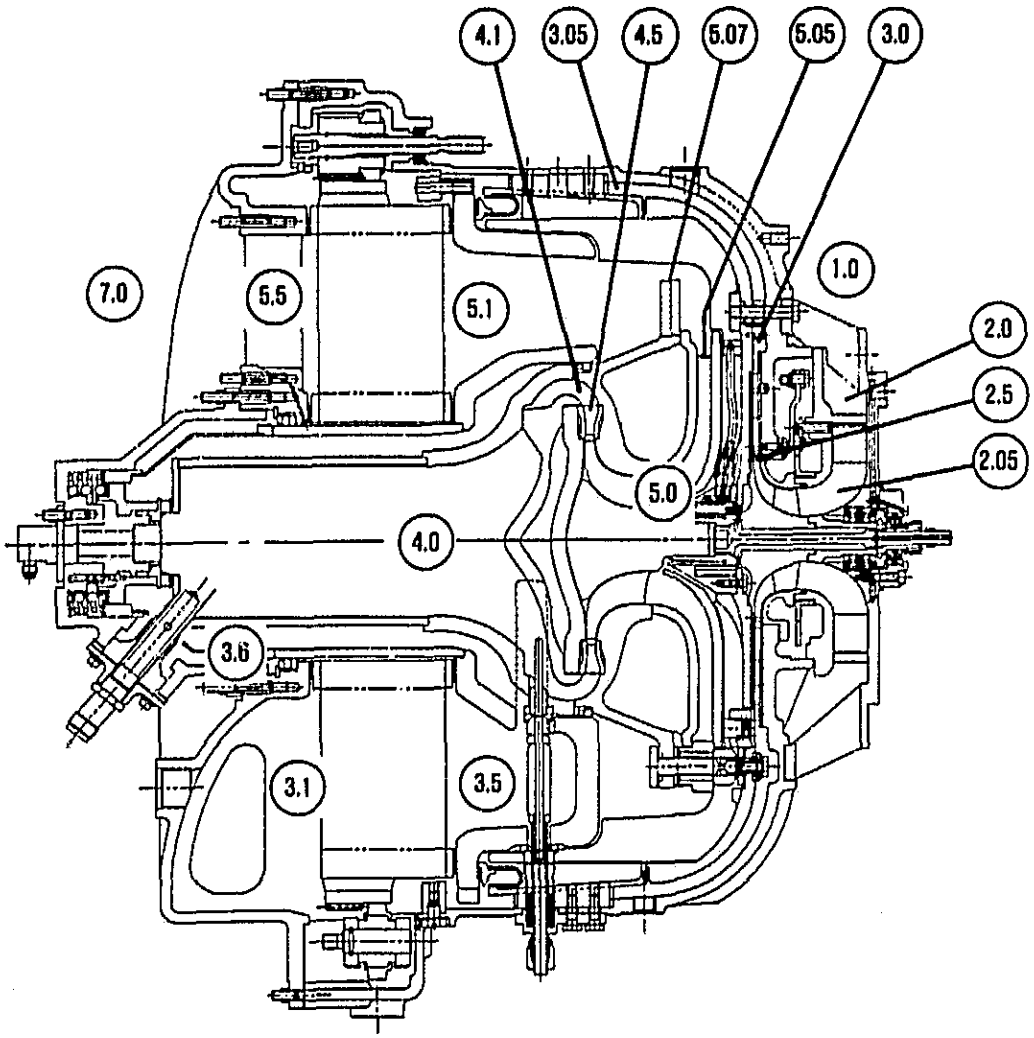

Figure 9. Performance Rating Stations.

TABLE 2. GEOMETRIC DESIGN SUMMARY

	Test 2A	SLE
Hub/Tip	0.4478	0.4478
Inlet Hub Radius (inch)	0.600	0.600
Inducer Sweep Angle (cold), degrees	7.28	7.37
Splitter LE Sweep Angle (cold), degrees	-5.43	-2.95
Exit Radius, inch	2.198	2.182
Exit b-Width, inch	0.1718	0.1718
Blade Number (inlet/exit)	12/24	12/24
Average Exit Blade Angle, degrees	50.71	47.97
Exit Rake Angle, degrees	0	0
Axial and Radial Clearance, inch	0.003	0.003
Inlet Shroud Normal Thickness, inch	0.015	0.015
Inlet Hub Normal Thickness, inch	0.025	0.025
Exit Shroud Normal Thickness, inch	0.015 (est)	0.014
Exit Hub Normal Thickness, inch	0.052 (est)	0.052
Average Exit Normal Thickness, inch	0.026 (est)	0.030
Vaneless Space Ratio	1.0751	1.0830
Diffuser Inlet Air Angles, degrees	73.09 (est)	72.87
Diffuser Inlet b-Width, inch	0.1664	0.1664
Diffuser Exit Radius, inch	3.233	3.233
Diffuser Exit b-Width, inch	0.134	0.134

TABLE 3. AERODYNAMIC DESIGN SUMMARY

	Test 2A Impeller	SLE Impeller
P/P_{Duct}, %	-1.8	-1.8
P/P_{IGV}, % From Test Data	-0.55	-0.55
$T_{T\ IN}$, R	544.7	544.7
$P_{T\ IN}$, psia	14.350	14.350
N_{PHYS}, rpm	100,000	100,000
W_{PHYS}, lbm/sec	0.855	0.855
Tip Speed, ft/sec	1918	1904
Total Temp Ratio	1.740	1.745
Efficiency, %	85.3	84.9
Specific Speed, rpm x 100	56.0	56.2
M_{rel} shroud	1.145	1.151
W_2/W_1 shroud	0.595	0.581
V_1 shroud / $V_{mean\ inlet}$	1.211	1.234
Average Deviation degrees	6.12	6.52
Slip Factor	0.8970	0.8921
Q(CAPS)	0.9360	0.9337
Pressure Ratio	5.625	5.663
Inlet Blockage	0.98	0.98
Exit Blockage	0.90	0.90

Table 3 shows an aerodynamic comparison. Duplication of the Test 2A impeller exit blade angle distribution could not be fully accommodated using SLE methodology. For example, to keep the same hub and shroud blade angles in the exit region resulted in an average exit blade angle less than Test 2A impeller. This lower exit blade angle gives rise to a lower slip factor and higher work for the same tip diameter. Therefore, the tip radius was reduced from 2.198 to 2.182 inches to compensate for the reduction in average exit blade angle from 50.71 to 47.97 degrees. Blade loadings are shown in Figures 10 through 12. All other salient design features were satisfactorily perserved using the SLE technique.

4.2 Turbine

The modified blading design has been released to the subcontractors for tooling. No other activity was addressed during this reporting period.

4.3 Combustion

Development of the backup diffusion flame combustor (DFC) was initiated for the S/N 002C ceramic engine. This combustor is a conventional film cooled, metal, design, and dis-

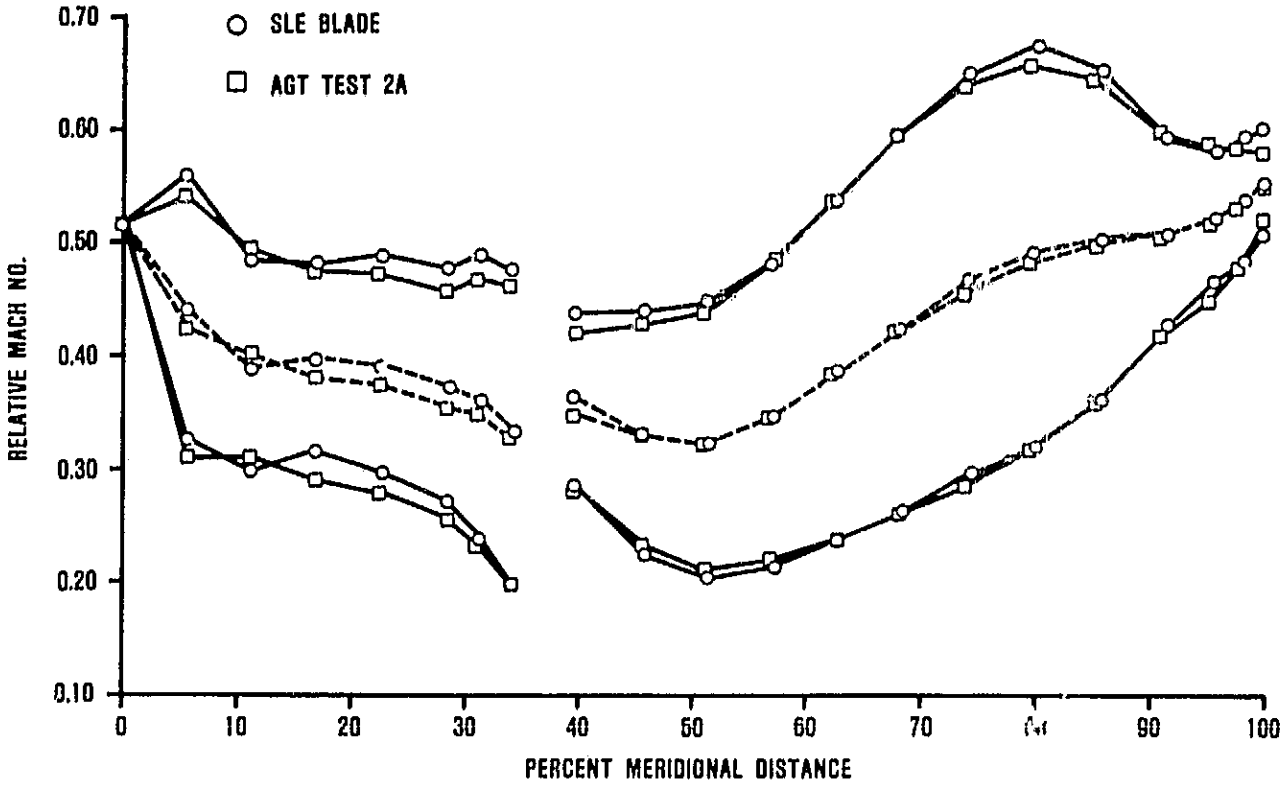

Figure 10. Impeller Blade Loading-Hub.

charge temperature rated at 2100°F. It is similar to the combustor used in the metal engine (1600°F TIT) except that the air orifices are proportioned to account for the different operating conditions.

Testing was conducted at idle and full load conditions. At the full load condition, the combustor maximum wall temperature was approximately 1800°F and uniform, while combustor discharge temperature pattern factor was within acceptable limits, 0.11. At idle, wall temperatures also were uniform with a maximum of 1800°F.

Ignition data was obtained by rig simulation at 15-, 25-, 35- and 45-percent speed points. Figure 13 shows the ignition data. Ignition fuel-air ratios linearly vary with engine speed and are 0.012 at 15-percent speed and 0.007 at 45- percent speed.

Nozzle Development

Test facilities down-time resulted in test program delays. The major contributing component was the second stage air pre-heater suppling the high temperature nonvitiated air to the test section. A natural gas slave preheater was designed and fabricated while repairs were accomplished. The backup is considered unsatisfactory for combustion testing wherein emissions are to be measured. However, for other parameters of importance such as nozzle integrity liner wall temperatures and lean blowout limits, it is a valid technique.

A film cooled version of the lean burn Simplex fuel nozzle has been received from Delavan (Figure 14). This nozzle is the result of a heat transfer analysis to establish sufficient air cooling techniques to suppress the onset of plugging as previously reported in Reference 7.

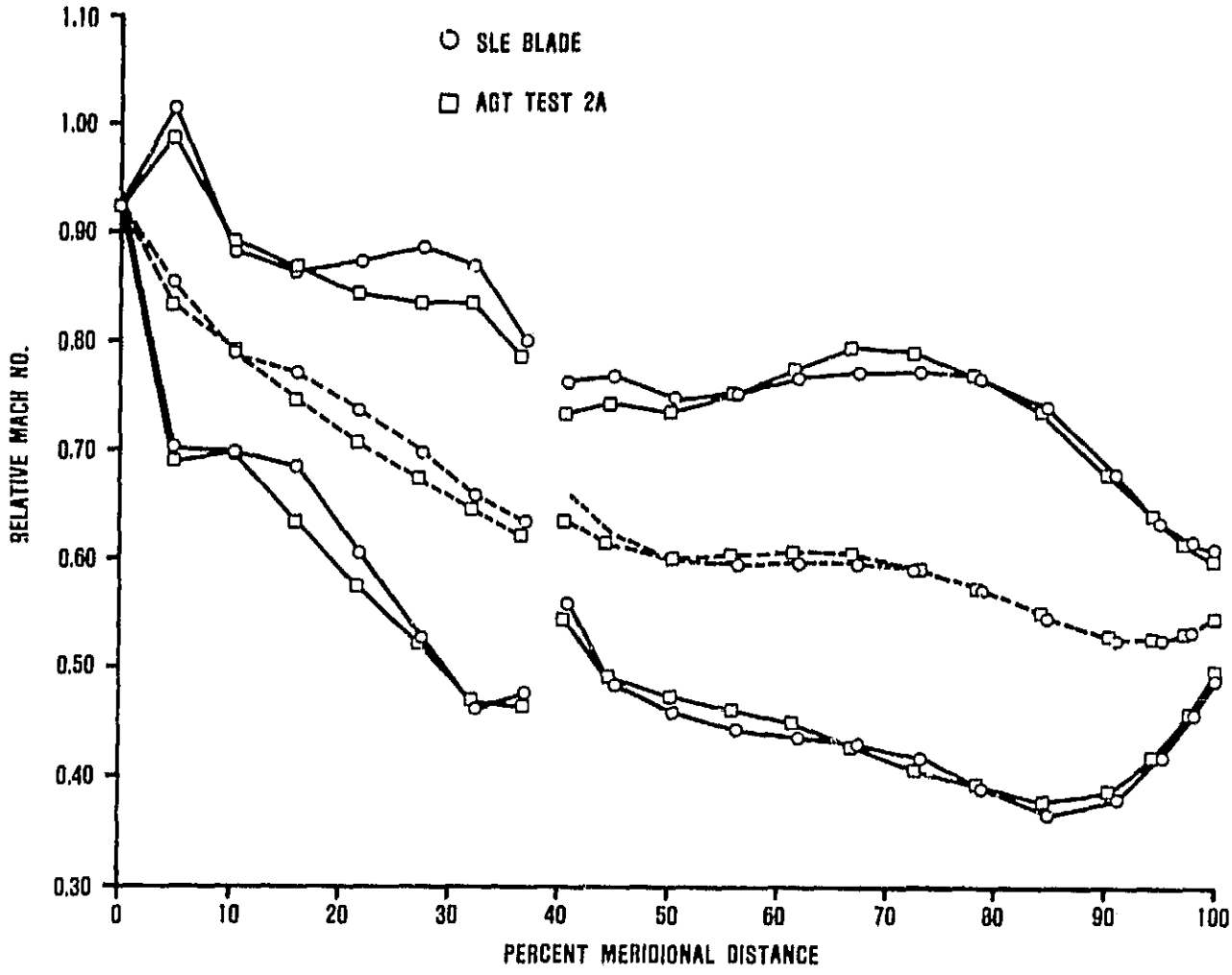

Figure 11. Blade Loading-Mid-Passage.

A back-up fuel nozzle design was implemented in collaboration with Delavan Corporation. The objective of this design (shown in Figure 15) was simplicity and compactness so as to maximize the cooling capability and minimize factors encouraging fuel coking. As shown, the design replaces the center body-swirler of the Simplex.

4.4 Regenerator Development

4.4.1 Ford Regenerator Development

4.4.1.1 Regenerator Cores

Samples of a new rectangular matrix with 1100 cells/in^2 were received from NGK. The modulus of rupture (MOR) is equivalent to the original thick-wall Isosceles triangular structure. The first full-size core with this matrix geometry also was received during this reporting period. In addition, three Corning thin-wall cores were received at Ford.

4.4.1.2 Regenerator Seals - Cooled Diaphragms

To accommodate the higher operating temperatures associated with the AGT101 (2500^{o}F) engine, the regenerator inboard (hot) seal crossarm requires diaphragm cooling. This design (Figure 16) has a funnel incorporated in the crossarm end diaphragm, allowing cooling air to flow between

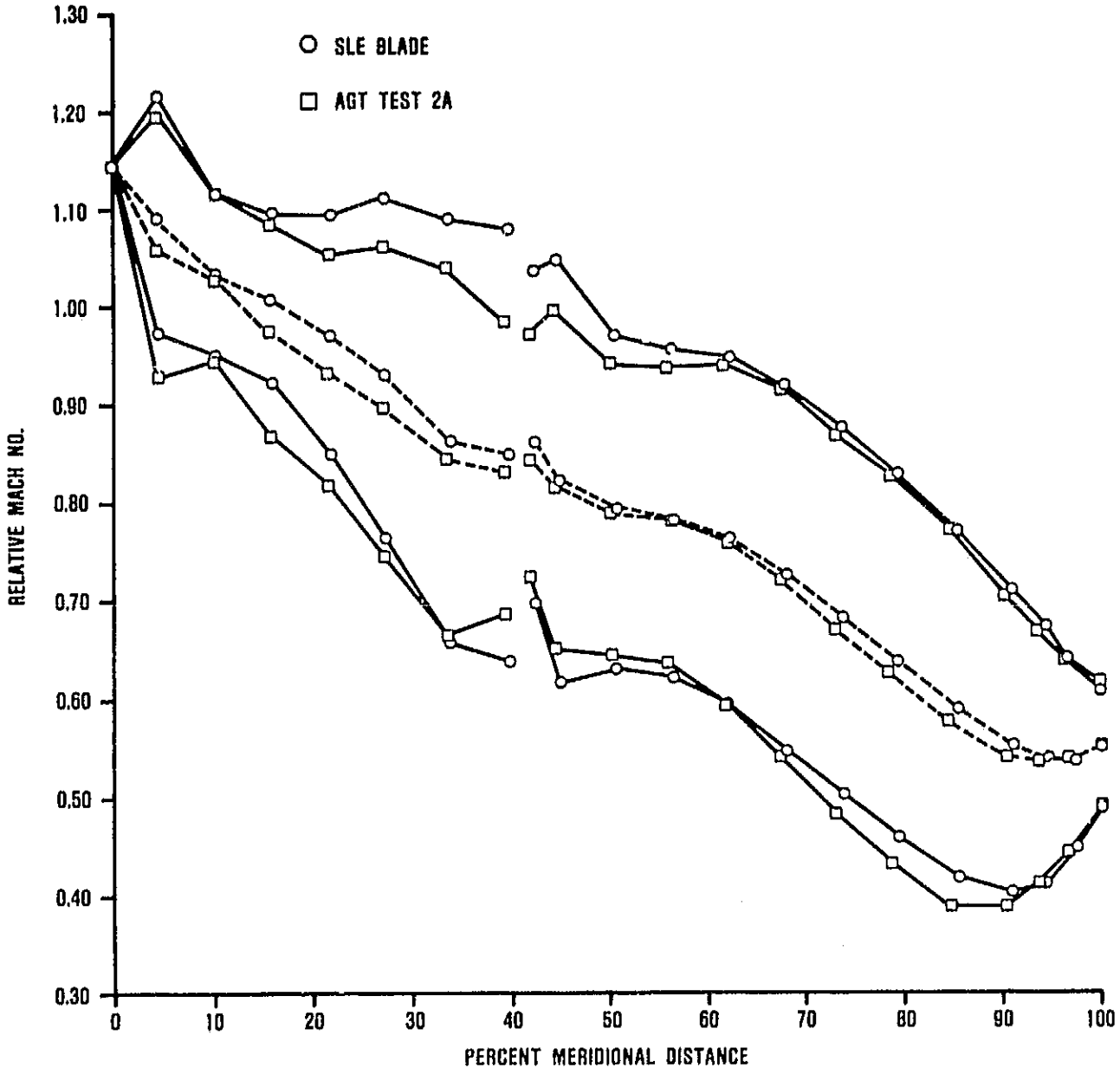

Figure 12. Impeller Blade Loading - Shroud.

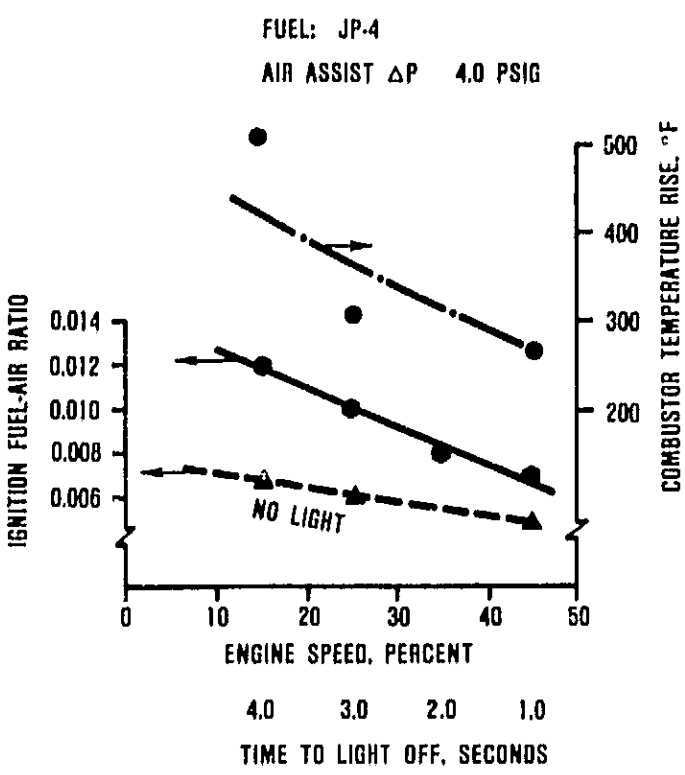

Figure 13. Diffusion Flame Combustor Ignition Performance.

the middle and lower diaphragms. A transfer tube at the corner allows the air to continue through the high pressure side of the inner periphery, exiting into the regenerator HP discharge air stream through holes in the middle diaphragm.

The initial inboard cooled diaphragm regenerator seal was evaluated in the ceramic structures rig at Garrett (Section 4.5.3 herein). Thermocouples were attached to both halves of the crossarm shoe and middle diaphragm. The design objective is to keep the diaphragm temperature below 1600°F. The results (Figure 17) indicated excellent cooling at the crossarm outer extremities with inadequate cooling air at the center hole region. The cooling passages and/or cooling flow control devices require additional work in this region to increase cooling flow.

To supplement the test hardware, a Ford/Honeywell Computer System Program for three-dimensional heat transfer analysis is being utilized. A parametric study will be conducted in an attempt to simulate the test temperatures to guide future design iterations.

4.4.1.3 Regnerator Seals - Performance Development

The main objectives for the Phase IV seal design were to maintain the leakage characteristics associated with the Phase III design with a reduction in mechanical load characteristics to reduce drive torque requirements. Several modified versions of the Phase IV seal design were fabricated during this reporting period for evaluation in the hot regenerator rig at Garrett. The intent of these seal combinations was to determine the effect of adjusting seal system loads on core operating position and resulting leakage and drive torque variations.

Three different combinations of the Phase IV seal design were evaluated in the hot regenerator rig. The best of these combinations was then selected for evaluation at various build clearances to determine the effect of diaphragm clearance on leakage and drive torque.

These seals were evaluated for a total diaphragm clearance variance of 0.052 to 0.077 inch. The leakage level for the Phase IV seals (Figure 18) was equivalent to the Phase III seals, Reference 7, even though the diaphragm clearance was 0.012 to 0.037 inch higher. In addition, the Phase IV seal had the cooling air funnel beneath the crossarm support diaphragm, which permits additonal leakage.

Drive torque requirements for the Phase IV seal design were significantly higher as illustrated on Figure 19. These data emphasize the need to incorporate a yoke at the fixed roller location to allow increased drive torque capacity for the present seal designs. This requirement will be reviewed with Phase V designs now in progress.

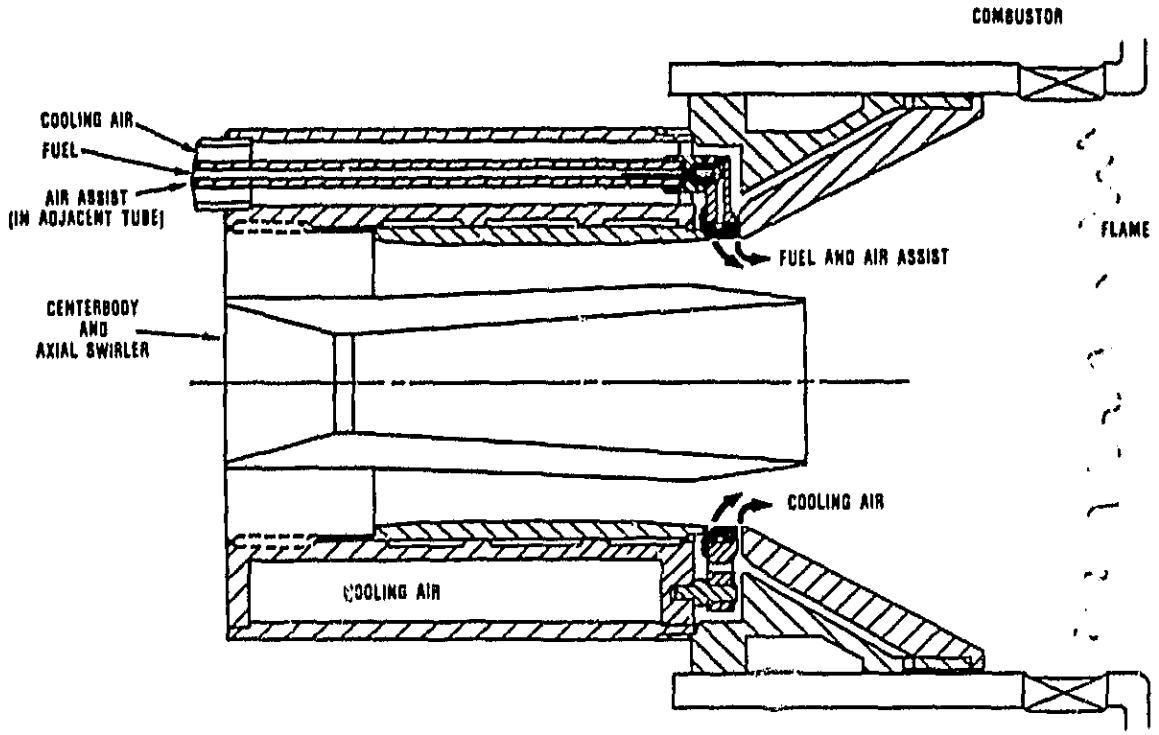

Figure 14. Simplex Mod II Fuel Nozzle (Film Cooled).

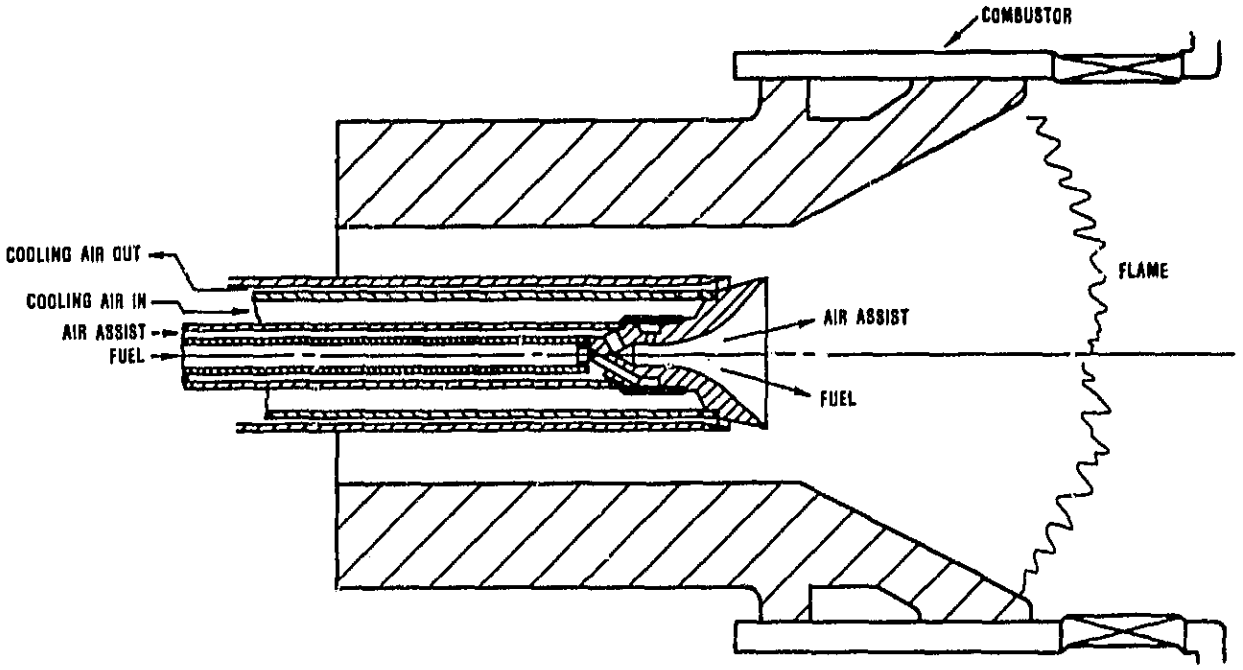

Figure 15. Simplex Fuel Nozzle (Delevan Corporation).

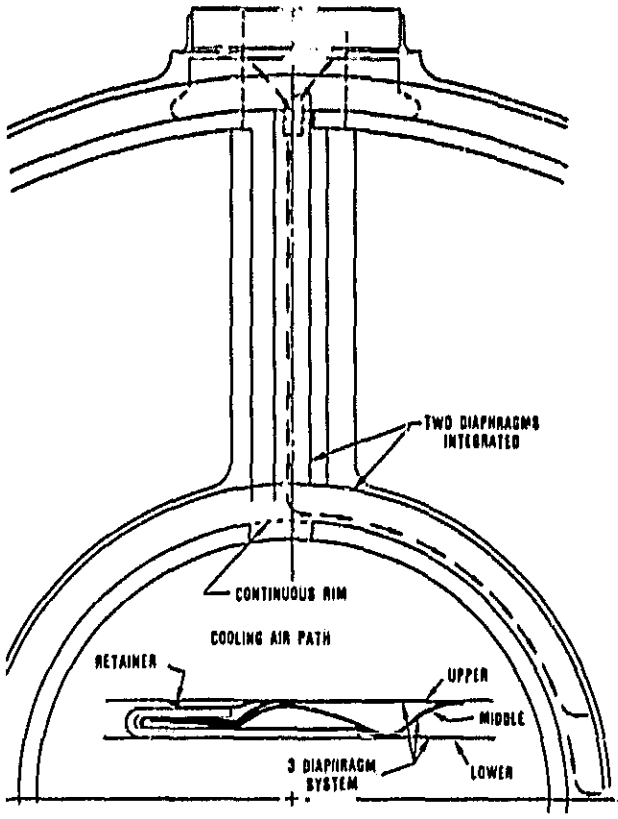

Figure 16. Cooled Regenerator Seal Schematic, Phase 4.

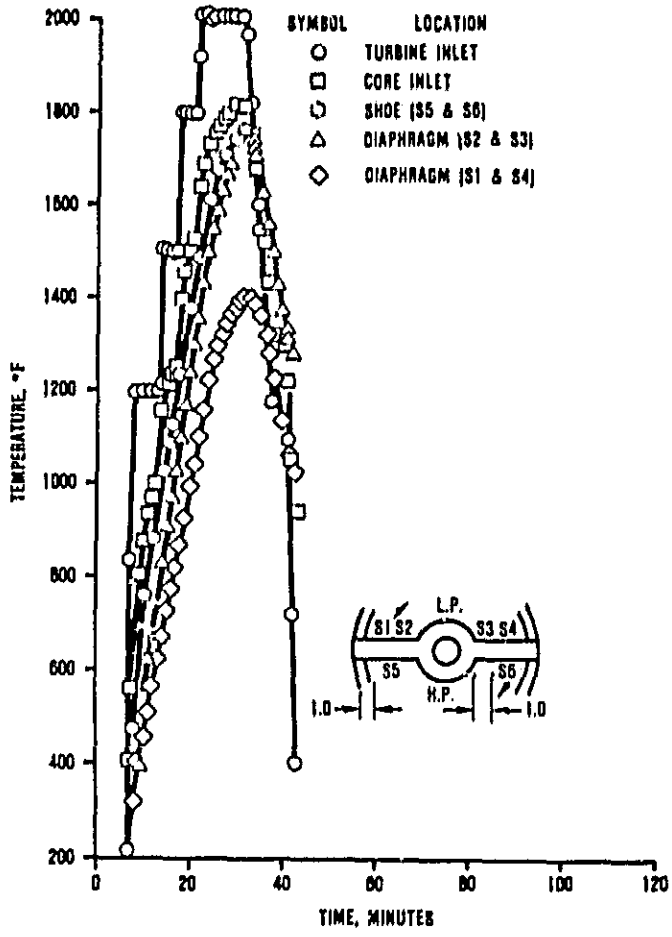

Figure 17. Regenerator Inboard (HOT) Seal Crossarm Temperature.

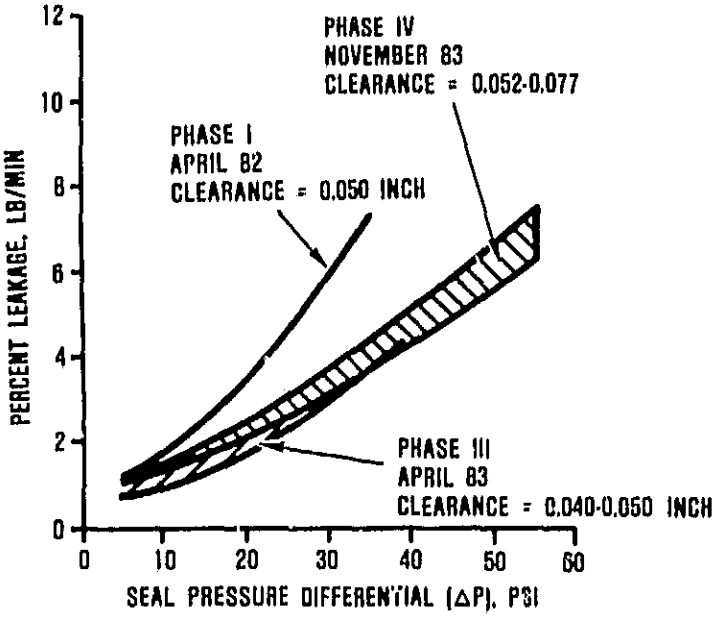

Figure 18. AGT Regenerator Seal Leakage.

Based on the test results for the Phase IV seal design, a Phase V design was initiated. The primary design objectives for the Phase V seal configuration were to decrease leakage and drive torque requirements. To accomplish these objectives, the Phase V design features an integrated crossarm diaphragm which eliminates the inner secondary diaphragm required in previous designs. A controlled test sequence in the static seal rig indicated a significant portion of the total leakage occurs at the inside and outside corners. In addition, the integrated crossarm diaphragm has a reduced lift angle, which should significantly reduce the mechanical load characteristics and drive torque requirements.

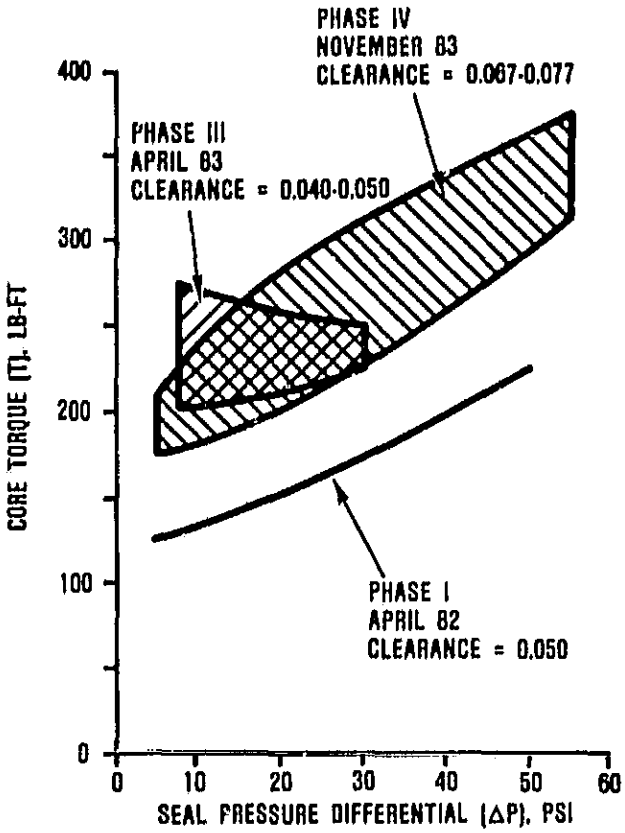

Figure 19. AGT Regenerator Core Torque.

The initial set of Phase V seals were fabricated for evaluation in the static seal rig. This seal design demonstrated a significant reduction in leakage level and sensitivity to diaphragm clearance (Figure 20) when compared to the Phase III and IV.

The mechanical load characteristics for the Phase V seal also indicate a significant reduction when compared to the Phase III and IV configuration as shown on Figure 21. Thus, the Phase V configuration exhibits potential for reduced leakage and drive torque characterisites. This set of seals will be evaluated in the hot regenerator rig during the next reporting period.

A new top plate for the static seal leakage rig was designed and fabricated during this report period. This plate has an opening in the plexiglass portion of the low pressure side to

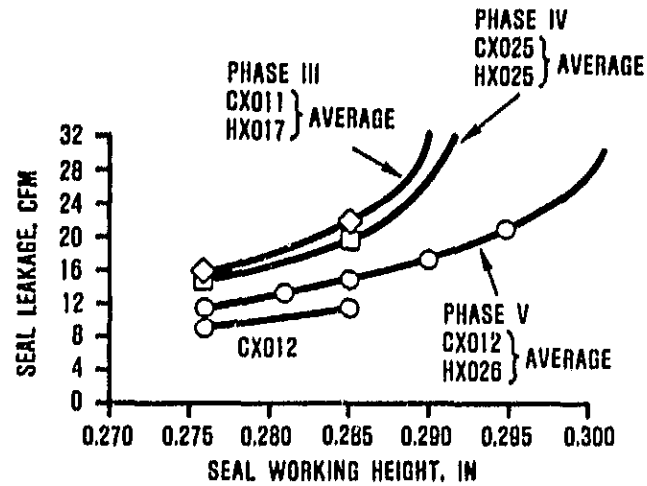

Figure 20. Leakage and Sensitivity Improvements of Phase V Seals.

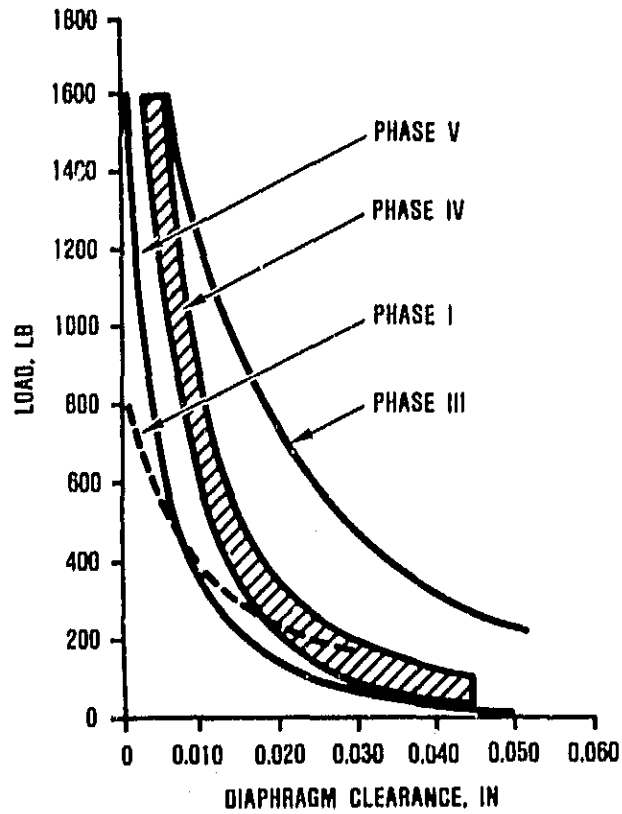

Figure 21. Regenerator Seal Mechanical Load.

accommodate detection of leakage between system components such as rubbing shoe, retainer and diaphragms.

Based on visual observation of coatings and diaphragms of previous seals tested in the AGT regenerator rig and engines, a significant leakage path appeared to occur in the center hole region. Consequently, definition of the cover and flow separator housing deflection as it effects seal pocket depth in this region is an important criterion for design improvements.

4.4.2 Regenerator Development (Garrett)

The hot regenerator rig was assembled and tested to evaluate the leakage characteristics and drive torque requirements of Ford's Phase IV regenerator seals.

Ford fabricated three sets of seals for test evaluation:

- o Baseline Phase IV seals
- o Phase IV with increased inner peripheral seal loading plus tapered thickness hot crossarm shoe
- o Phase IV with increased seal loading plus welded seal diaphragms

Each of these seal sets were installed and tested in the hot regenerator rig under nominal operating conditions ($T_{3.1} \approx 250^{o}F$, $T_{5.1} \approx 1200^{o}F$).

The third seal set with welded diaphragms exhibited such high seal loading resulting in excessive drive torque and prohibited the measurement of useful data. In fact, while attempting to test these seals, the ring gears were separated from two regenerator cores as a result of drive torques in the 300 to 450 ft-lb range.

Successful tests were completed on the baseline and tapered seal sets. The drive torque and leakage characteristic for these seals are shown on Figures 22 and 23, respectively.

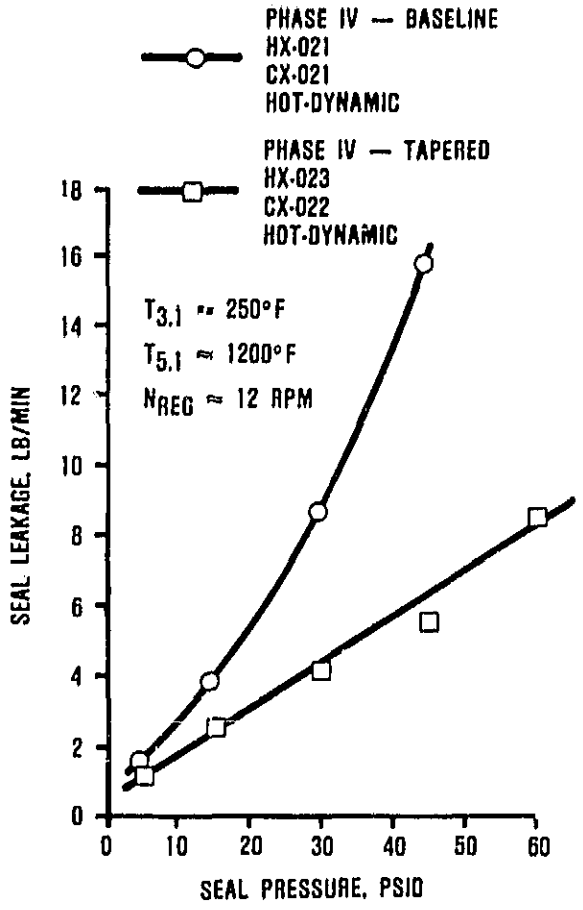

Figure 22. Regenerator Seal Leakage.

The baseline seal set exhibited lower drive torque requirements and substantially higher leakage than the tapered seal set. The disparity in seal performance is probably a result of the higher seal stiffness of the tapered seal set.

Relative to the best of the earlier seal configurations neither of these seal sets exhibited an improvement.

Instrumentation was added to this rig to measure the variations in seal clearance at the regenerator seal inner periphery crossarm positions. This instrumentation consisted of a set of Bently clearance probes mounted on a bracket anchored to the exhaust cover bolt circle. The Bently targeted a "finger" fixed to

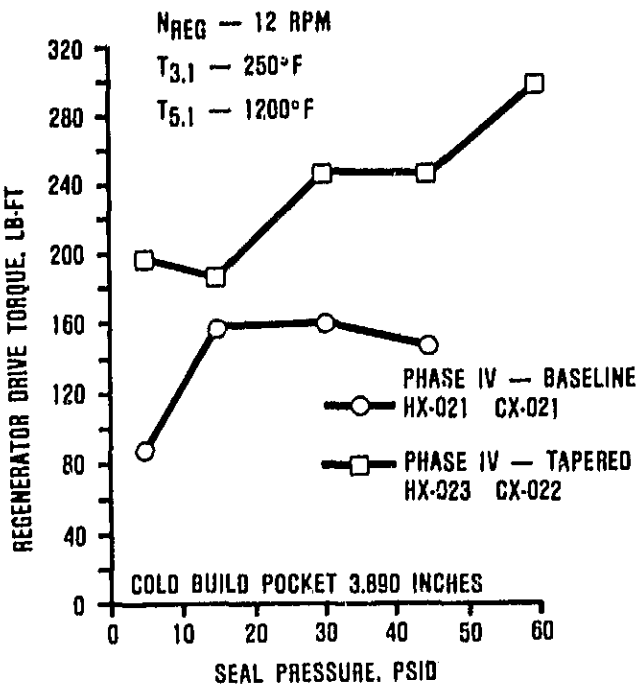

Figure 23. Regenerator Drive Torque.

the regenerator shield. Another Bently targeted the flat land of the exhaust cover. This system is shown in Figure 24. By comparing these clearance measurements, taking into account thermal growth of the regenerator shield, and the thermal effects on the Bently calibrations the local variations in regenerator pocket can be calculated.

The data from this clearance probe instrumentation was inconclusive due to the lack of information on the thermal growth of the regenerator shield. Qualitatively however, these data seemed to indicate an opening of the inner peripheral regenerator pocket with increased rig pressure.

This test will be repeated at a future date with more comprehensive thermal instrumentation on the regenerator shield.

4.5 Ceramic

4.5.1 Materials

4.5.1.1 Ceramic Material Testing Summary

A summary of the material property results is presented in Table 4. Additionally, a material characterization reference chart, indicating where additional information (generated by Garrett), is presented in Table 5.

4.5.1.2 Turbine Diffuser/Insulation Evaluation

As reported previously, (Reference 7), the use of a fibrous insulation system as a portion of the turbine diffuser design was stimulated by results of the Babcock and Wilcox vacuum-formed 3000 material insulation in Builds 9 and 10 of the structures rig. Results of that testing supported the ability of this type of insulation to withstand high temperature gas velocities for short durations. However, surface erosion on the insulation indicated that a more durable system would be required for longer term exposure and higher gas velocities. In pursuit of an improved insulation system, several samples of Lockheed High Temperature Protection (HTP) were obtained for evaluation. The sample consisted of cylinders of sintered and machined high purity SiO_2 and Al_2O_3 fibers. The samples were machined to form cylinders with a 3.1-inch bore and a 3-inch length. As machined cylinders, and cylinders partially coated with a borosilicate glass, designated by NASA and Lockheed as reaction cured glass (RCG), were provided by Lockheed and shown in Figure 25.

Two samples, one uncoated and one coated, have been exposed to combustor discharge gases as illustrated in Figure 26. During this test, vitiated air at 2100°F was directed through the cylinder bore at 20 lb/min (approximately 250 ft/sec) for 46 minutes. This condition exceeded the 75 ft/sec gas velocity predicted for the turbine exhaust diffuser dump region currently utilizing the Babcock and Wilcox fibrous insulation.

Post test visual examination did not reveal any damage to the coated sample and only minor surface erosion on the uncoated sample.

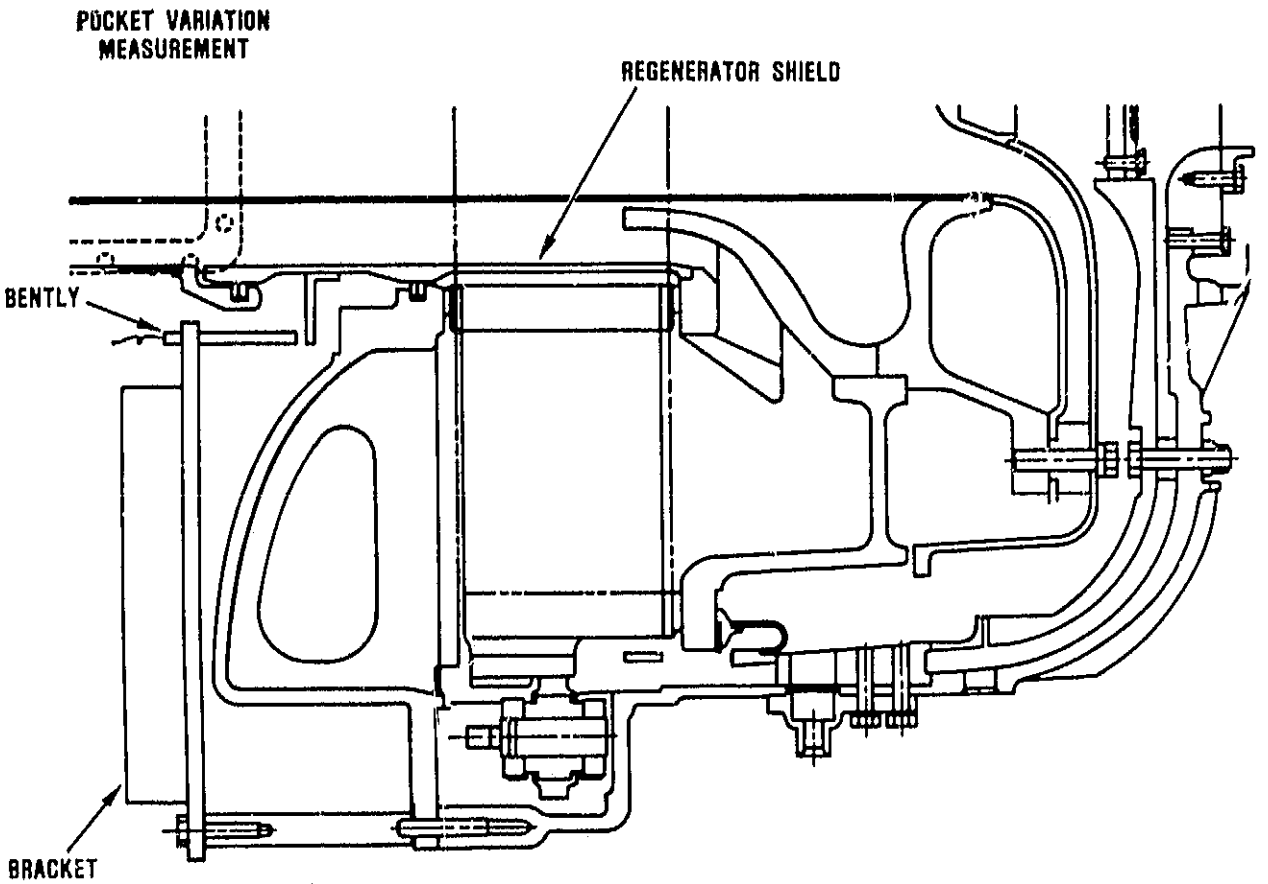

Figure 24. AGT Hot Regenerator Rig.

TABLE 4. AGT101 COMPONENT AND MATERIAL SUMMARY

Supplier	Material	Process	Condition	Qualification Bar							Ceramic Component						
				Room Temperature			Elevated Temperature				Room Temperature			Elevated Temperature			
				σ_θ [4]	M	Population	σ_θ [4]	M	°F	Population	σ_θ [4]	M	Population	σ_θ [4]	M	°F	Population
ACC Inner Diffuser Outer Diffuser Turbine Shroud	RBSN (RBN104)	Slip Cast	As-Fired Longitudinally Ground Heat Treated	49.7 53.2 54.8	4.5 5.5 8.5	30 10 29	52.1	10.1	2200	10	44.3 [6] 46.3	8 5.3	21 27	-- --	-- --	-- --	-- --
ACC Stator	RBSN (RBN124)	Injection Molded	As-Fired [1]	40.1	4.8	19	44.5	8.4	2200	23	--	--	--	--	--	2200	--
ACC Rotor	Sintered Si_3N_4 (SNN 502)	Slip Cast	Longitudinally [2] Ground	--	--	--	--	--	--	--	113 [3]	16.6	20	54	9.5	--	10
	Sintered Si_3N_4 (SNN 522)	Injection Molded	As-Fired	89.2	8.9	30	80.9 66.1 67.5 25.6	7.6 11.1 10.8 13.6	1880 2000 2200 2500	9 30 10 12	--	--	--	--	--	--	--
Carborundum Turbine Shroud, Stator	Sintered α-SiC	Injection Molded	As-Fired	48.6	9.5	30	45.0	5.0	2500	10	55.6 [5]	7.1	9	--	--	--	--
Combustor Baffle	Sintered α-SiC	Slip Cast	Longitudinally Ground	49.4	5.8	30	41.4	6.7	2500	10	53.0	7.3	9	--	--	--	--
Transition Duct, Regen Shield, Back-shroud	Sintered α-Sic	Isopressed	Longitudinally Ground	57.7	7.7	30	56.2	11.9	2500	10	--	--	--	--	--	--	--
Ford Rotor	SRBSN (RM-2)	Slip Cast	Longitudinally Ground	109.3	19.8	6	73.1	16.4	2200	6	--	--	--	--	--	--	--
Stator	RBSN	Injection Molded	As-Fired	43.1	9.2	39	45.8	7.7	2200	10	--	--	--	--	--	--	--
NGK Backshroud, Transition Duct	Sintered Si_3N_4 (SN-50)	Isopressed	Longitudinally Ground	87.6	10.5	10	47.1	13.6	2000	7	--	--	--	--	--	--	--

All test bars 0.250 x 0.125 inch cross section unless noted. Bars tested in 4-point flexure, 1.50 inch outer span and 0.75 inch inner span. Cross head speed, 0.02 inch/minute

[1] Test bar cross section 0.31 x 0.15 inch

[2] Test bar cross section 0.2 x 0.1 inch

[3] 98.8 percent dense

[4] Characteristic strength, ksi

[5] As machined, longitudinally ground

[6] Test bar cross section 0.236 x 0.1 inch

This erosion was judged a result of local surface damage resulting from the machining operation rather than the exposure conditions. These preliminary results indicate that coated or uncoated HTP may be suitable for use in the current AGT101 engine configuration and that the RCG coated HTP may be suitable for use in higher gas velocity locations. Procurement of additional test articles and additional testing will be pursued.

4.5.2 AGT101 Ceramic Component Thermal Screening

Prior to qualification testing of AGT101 ceramic components in the static structures rig, all ceramic parts with predicted high thermally induced stress are screened in subassembly thermal screening rigs.

Thermal screening is intended to eliminate components with gross internal defects and/or smaller defects located in regions of high bending or tensile stress. These lower quality components will fracture during thermal screening allowing only the highest quality parts to continue through qualification testing and subsequent engine tests. The thermal screening rigs provide a screening test bed for various components, configurations, and material changes and have an upper temperature limit of 2100°F.

TABLE 5. SUMMARY OF AGT CERAMIC MATERIAL CHARACTERIZATION AT GARRETT.

	AiResearch Casting Co.				Carborundum Co.							Corning	Ford Motor Co.			NGK Locke	Pure Carbon
	Reaction-Bonded Si_3N_4		Sintered Si_3N_4		Sintered SiC			Reaction-Sintered SiC				LAS	SRBSN	RBSN	LAS		
	SC	IM	SC	IM	SC	IM	IP	CP	CM	IP	Hot Pressed SiC		SC	IM		IP	IP
	RBN-104	RBN-124 RBN-126	SSN-502	SSN-522					KX-01	KX-02			RM-2			SN-30	Refel
Flexure Strength																	
Room Temperature	S1-245 S7-S6-96	S1-251	S3-46	S1-256	S2-61 S6-97	S1-266 S6-99	S1-263	S1-264 S7-59				S6	S4-28	S2-68	S6		
Elevated Temp, T_1 (1800-2000°F)		S1-251		S1-256				S1-264	S3-51	S4-25		S6			S6	S3-45	
T_2 (2200°F)	S1-245			S1-257				S2-59 S1-264					S4-28	S2-68			
T_3 (2500°F)	S1-245	S1-251		S1-258	S2-61	S1-266	S1-263	S2-59 S1-264						S2-68			
Transverse Machined	S1-248			S1-255				S2-58 S1-277									
Longitudinal Machined	S1-248			S1-255		S1-266		S1-277	S3-51	S4-25			S4-28			S3-45	S3-48
Cut from Components	S6 CCM81		S3-46 S4				S2-87				S3-49						S3-48
Post-Machining Oxidation	S1-248 S7				S2-61			S2-59 S1-277		S4-25							S3-48
Oxidation																	
Gradient Furnace				S4-30									S4-30				
Dynamic Durability Rig	*							*					S4-38				*
Stress Rupture																	
Static, Air			S6-	S4-31 S1-262 S2-63									S4-31				
Dynamic, Gas Fired	S2-65							S2-65									
Interface Considerations																	
Compatibility Test	S5-38 CCM82				S5-38 CCM82	S5-38 CCM82		S5-38 CCM82	S5-38 CCM82			S5-38 CCM82				S5-38 CCM82	
Sliding Tests	S2-74 S1-281							S2-75									
Coating Development	S2-78 S1-280							S2-78									
Shrink Fit/ Ratchet Tests																	
Thermal Shock (Stator)		S4-35				S4-35											
Spin Test (Rotor)																	
Bladeless Rotor			S3-46			S2-85	S2-85						CCM81				S3-48
Bladed Rotor			S5-35										CCM82				

*Tested under NASA 3500-Hour Durability Program, Contract DEN3-27.

SC = Slip Cast
IM = Injection Molded
IP = Isopressed
CP = Cold Pressed (Uniaxial)
SRBSN = Sintered Reaction Bonded Si_3N_4

Examples of References:

S1-245 = Page 245, First Semi-Annual Report

CCM82 = Paper presented at 1982 CCM

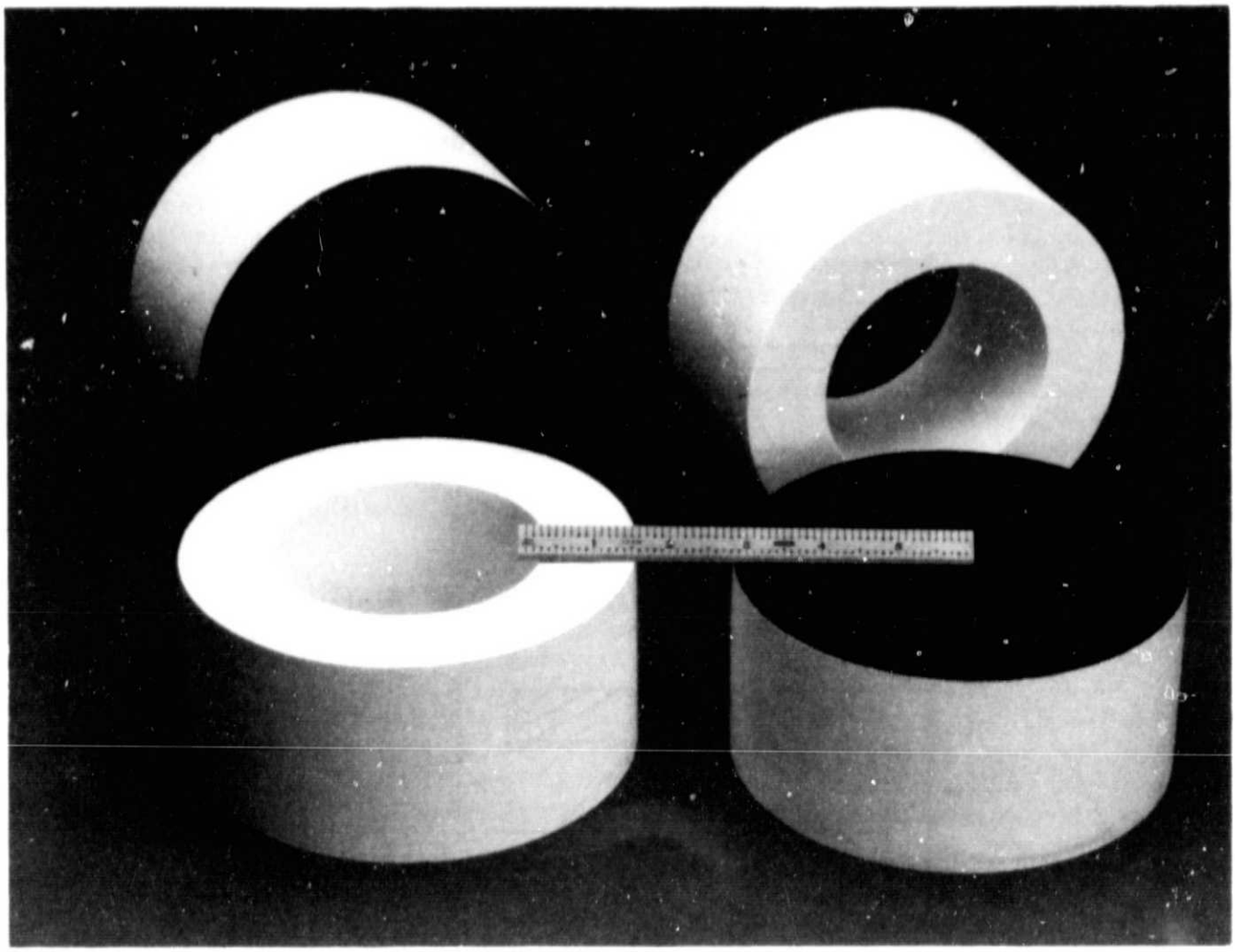

Figure 25. RCG Coated and Machined HTP Insulation From Lockheed.

A list of the AGT101 ceramic static structural components tested during this reporting period are shown in Table 6. These tests have successfully screened components to 2100°F and have provided valuable data for stress reduction design modifications.

During this reporting period, experimentation with improved screening rig insulation, using vacuum formed alumina-silica fiber, was conducted. The goal is to extend the life of the screening rigs while duplicating, as closely as possible, engine thermal conditions.

An improved insulation configuration for the transition duct and combustor baffle screening rig was successfully employed in the December 8 1983 test of these components. Figure 27 illustrates the old and new configurations. It is anticipated that the life of this rig be significantly extended.

The turbine shroud/turbine stator/turbine backshroud screening rig was likewise upgraded to a new insulation configuration, as illustrated in Figure 28. The more effective insulation and alteration of the flowpath are felt to have contributed to higher shroud stresses, and subsequent fracture of turbine shrouds S/N 377 and S/N 374 on December 5 and December 12, 1983 respectively (Table 6). Review of S/N 216 is underway.

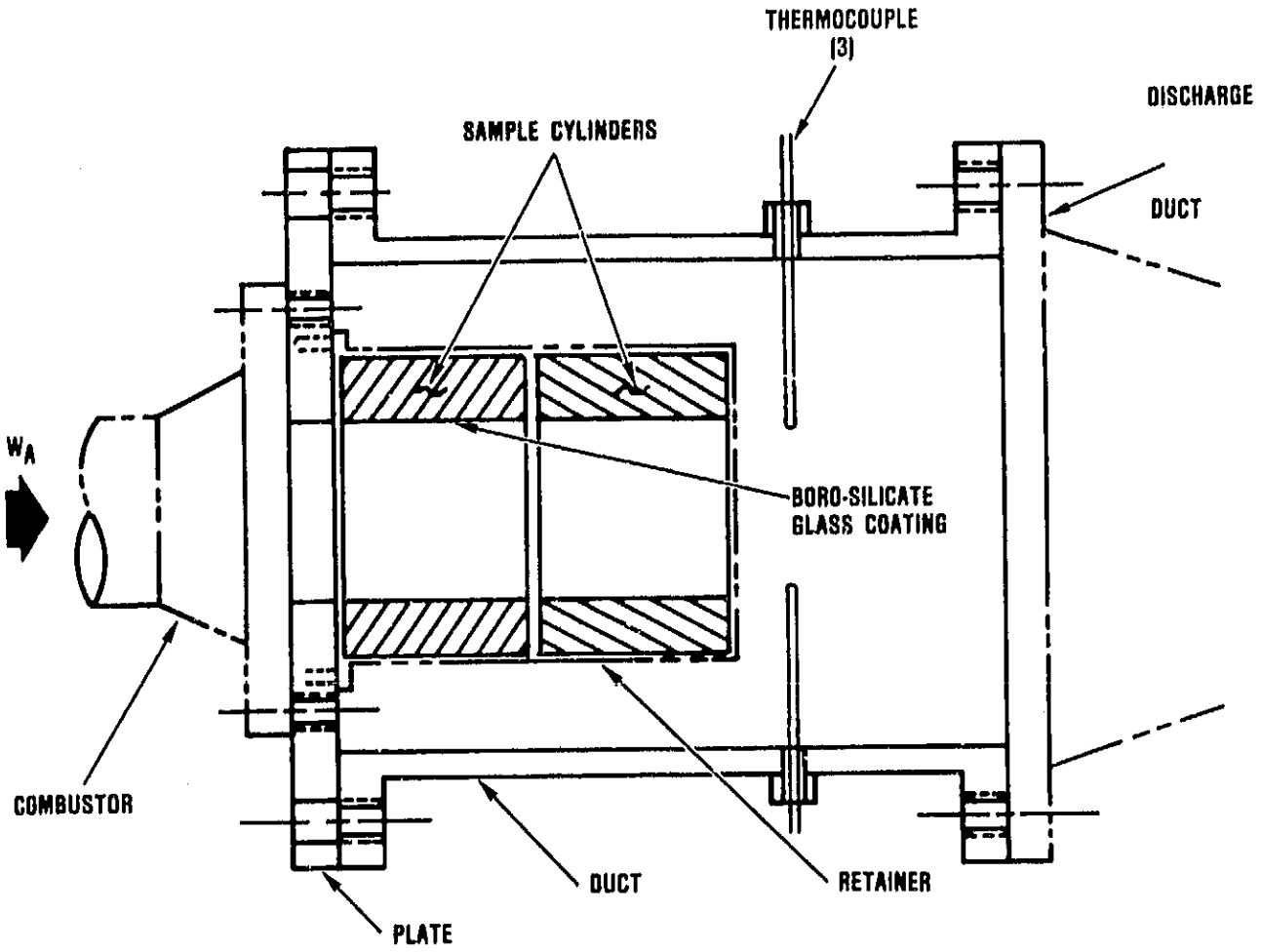

Figure 26. AGT101 Insulation Test Rig.

4.5.3 Ceramic Structures Rig Testing

Build 7

Build 7 was initiated in August 1983 with ceramic component hardware previously screened in individual and sub-assembly thermal and mechanical screening rigs. During the final stages of the assembly, as the spring loaded combustor and regenerator heat shield were being installed, the inner regenerator shield platform of the flow separation housing (FSH) fractured. Figure 29 illustrates the fracture region. Disassembly and inspection of the fractured component revealed the presence of an interference between the fillet and corner radii of the FSH and the regenerator shield.

The corner radii was increased to a larger value than the fillet radii in the mating part (replaced FSH for Build 8) and the rig was reassembled.

TABLE 6. THERMAL SCREENING SUMMARY

Date	Component or Sub-Assembly	S/N	Mat'l	Supplier	T_{max}, °F	Results
7/1/83	Inner Diffuser Housing	294	RBSN	ACC	2000	OK
	Outer Diffuser Housing	289	RBSN	ACC		OK
7/27/83	Transition Duct	002	SSN	NGK	2100	OK
	Combustor Baffle	112	SASC	CBO		OK
7/28/83	Transition Duct	111	SASC	CBO	2100	OK
	Combustor Baffle	111	SASC	CBO		OK
8/1/83	Turbine Shroud (B-3 Design)	307	RBSN	ACC	2100	OK
	Turbine Stators (Segmented)	Set 2	RBSN	ACC		OK
	Turbine Backshroud	002	SSN	NGK		OK
8/2/83	Turbine Shroud (B-3)	308	RBSN	ACC	2100	OK
	Turbine Stators (Segmented)	Set 3	RBSN	ACC		OK
	Turbine Backshroud	105A	SASC	CBO		OK
8/3/83	Inner Diffuser Housing	309	RBSN	ACC	2000	OK
	Outer Diffuser Housing	300	RBSN	ACC		OK
	Ceramic Bolt Assembly	007	HPSN	Norton		OK
		008	—	—		OK
		009	—	—		OK
	Ceramic Rocker Assembly	007	SASC	CBO		OK
		008	—	—		OK
		009	—	—		OK
8/9/83	Inner Diffuser Housing	311	RBSN	ACC	2000	OK
	Outer Diffuser Housing	297	RBSN	ACC		OK
	Ceramic Rocker Assembly	004	SASC	CBO		OK
		005	—	—		OK
		006	—	—		OK
10/4/83	Turbine Shroud (B-3)	354	RBSN	ACC	2100	OK
	Turbine Stators (Segmented)	Set 4	SASC	CBO		OK
	Turbine Backshroud	104	SASC	CBO		OK
12/2/83	Inner Diffuser Housing	318	RBSN	ACC	2000	OK
	Outer Diffuser Housing	334	RBSN	ACC		OK
	Ceramic Bolt Assembly	013	HPSN	Norton		OK
		014	—	—		OK
		015	—	—		OK

TABLE 6. THERMAL SCREENING SUMMARY (Contd)

Date	Component or Sub-Assembly	S/N	Mat'l	Supplier	T_{max},°F	Results
12/5/83	Turbine Shroud (B-3)	377	RBSN	ACC	2100	Fracture
12/8/83	Transition Duct	109	SASC	CBO	2100	OK
	Combustor Baffle	122	SASC	CBO		OK
12/12/83	Turbine Shroud (B-3)	374	RBSN	ACC	2100	Fracture
12/13/83	Inner Diffuser Housing	317	RBSN	ACC	2000	OK
	Outer Diffuser Housing	364	RBSN	ACC		OK

Build 8

On August 31, 1983 the AGT101 Ceramic Static Structures Rig successfully qualified a complete set of development engine static structural ceramic components through seven simulated engine start transients to 2000°F. A statistical summary of the test is shown below:

o Total Light-Offs	14
o Time at 1200°F	1 Hr 48 Min
o Time at 1500°F	44 Min
o Time at 1800°F	40 Min
o Time at 2000°F	1 Hr 26 Min
o Transient Time	1 Hr 3 Min
o Total Rig Time	5 Hrs 45 Min

The rig assembly included seventy-eight ceramic components fabricated from three basic materials; silicon nitride, silicon carbide, and lithium aluminum silicate (Table 7). Six fabrication processes were utilized representing the fabrication techniques and capabilities of six ceramic suppliers.

The simulated development engine start transient followed for this test is shown in Figure 30. Engine idle conditions for HP and LP airflows were maintained at 10 lb/min with a differential pressure of 5 psid. Figure 31 shows a typical $T_{4.1}$ trace during the test and Figure 32 depicts the LP regenerator inlet temperature ($T_{5.1}$) as a function of cycle time.

Rig testing was terminated during the eighth start transient due to excessive high pressure to low pressure internal leakage. The rig was disassembled and inspected for component damage.

Minor chipping was noted on the following components: combustor baffle strut, eccentric spacers, flow separator housing ID seal ring, and T4.1 (TIT) thermocouple load spacers. None of the noted chipping was a result of material interface sticking.

The regenerator inner seal (hot side seal) had temperature instrumentation installed to monitor both seal diaphragm and substrate temperatures. The excessive leakage that terminated the test was due to collapsed diaphragms on the inner seal from over-heating. The inner seal incorporated Ford's initial air cooled diaphragm design. Inspection of the failed seal indicated partial blockage of the cooling air passage from the installed instrumentation. Ford's heat transfer analysis shows that the seal should properly function when the cooling flow is unobstructed.

The vacuum formed ceramic fiber insulation used to form the diffuser discharge flow path survived the test with minor radial cracks (Figure 33) through the flowpath coating layer and substrate. The surface coating appears to have cracked and spalled off the substrate in the highest velocity region immediately downstream of the diffuser discharge. Radial

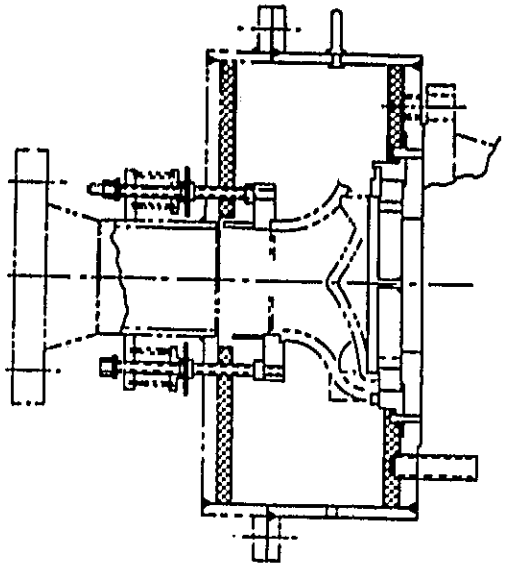

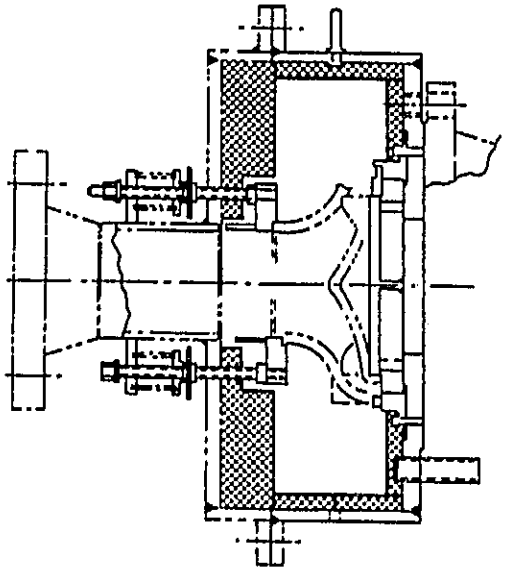

Figure 27. Transition Duct and Baffle Screening Rig With Previous (top) and Revised (bottom) Insulation Configurations.

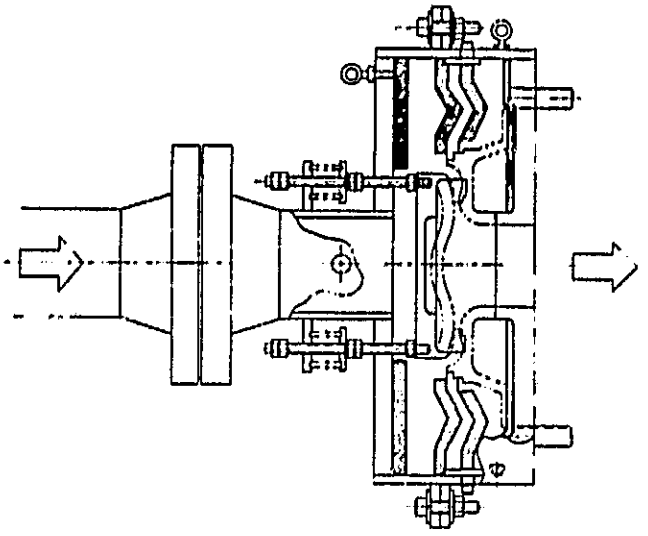

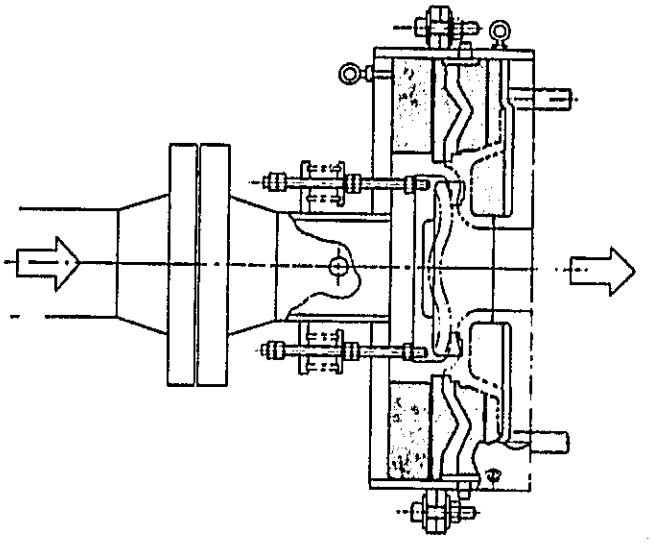

Figure 28. Turbine Shroud/Turbine Stator/ Turbine Backshroud Screening Rig With Previous (top) and Revised (bottom) Insulation Configuration.

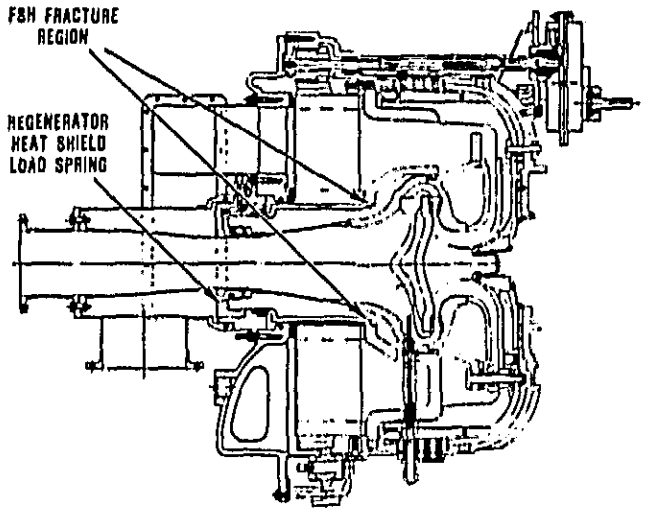

Figure 29. Fracture Region.

cracking in the substrate was evident in the high velocity region immediately downstream of the diffuser discharge, and appears to be related to the vacuum forming fabrication process. Large voids are evident between the "plate-like" layers of material which weaken the insulation mechanical properties. Improved fabrication techniques by the supplier are expected to alleviate the poor quality of the insulation preforms.

Turbine shroud alignment is of paramount importance in maintaining proper turbine rotor running clearance within close tolerances. The ceramic rocker/eccentric assembly successfully maintained cold assembly runout dimensions of 0.0015 inches Total Indicated Reading (TIR) through the cyclic testing.

TABLE 7. RIG ASSEMBLY CERAMIC COMPONENTS

Three Materials, Six Fabrication Processes, Six Suppliers

In B/N8

Component Name	S/N	Material	Source	Quantity	Design Configuration
Regenerator Shield	104	SASC	CBO	1	A-1
Regenerator Shield Piston Ring	001, 002	RSSC	Pure Carbon	2	A-1
Flow Separator, Housing	13	LAS	Corning	1	A-2 (3-$T_{4.1}$ Probes)
Regenerator Core		MAS	NGK	1	Coated Thick Wall
Transition Duct	111	SASC	CBO	1	A-3 (3-$T_{4.1}$ Probes)
Transition Duct $T_{4.1}$ Bushing	001, 002, 003	SASC	CBO	3	A-1
$T_{4.1}$ Inner Seal (Female)	001, 002, 003	LAS	Corning	3	A-1
$T_{4.1}$ Inner Seal (Male)	001, 002, 003	LAS	Corning	3	A-1
$T_{4.1}$ Inner Seal Spacer	001, 002, 003	LAS	Corning	3	A-1
$T_{4.1}$ Inner Seal Load Spacer	001, 002, 003	LAS	Corning	3	A-1
$T_{4.1}$ Outer Seal (Female)	001-004	LAS	Corning	4	A-1
$T_{4.1}$ Outer Seal (Male)	001-004	LAS	Corning	4	A-1
Combustor Baffle	112	SASC	CBO	1	A-2 (0.200 Wall-Uniform)
Turbine Backshroud	102	SSN	NGK	1	A-1
Turbine Stators (Seg.)	Set #2	RBSN	ACC	19	A-1
Turbine Shroud	308	RBSN	ACC	1	B-3
Turbine Shroud I.D. Seal	0.001	RBSN	ACC	1	A-1
Turbine Shroud Wave Spring	001	RBSN	ACC	1	A-1
Turbine Shroud O.D. Seal	001	RBSN	ACC	1	A-1
Outer Diffuser Housing	300	RBSN	ACC	1	A-3 (Dump Section)
Inner Diffuser Housing	311	RBSN	ACC	1	B-2
Inner Diffuser Load Spacer	001, 002, 003	LAS	Corning	3	A-1
Bolt Assembly	004, 005, 006	HPSN	Norton	3	A-1
Rocker	004, 005, 006	SASC	CBO	3	A-1
Eccentric	004, 005, 006	SASC	CBO	3	A-1
Contract Washer (Upper)	004, 005, 006	HPSN	Norton	3	A-2 (0.150 Thickness)
Contract Washer (Lower)	004, 005, 006	HPSN	Norton	3	A-2 (0.150 Thickness)
Crowned Washer	004, 005, 006	HPSN	Norton	3	A-1

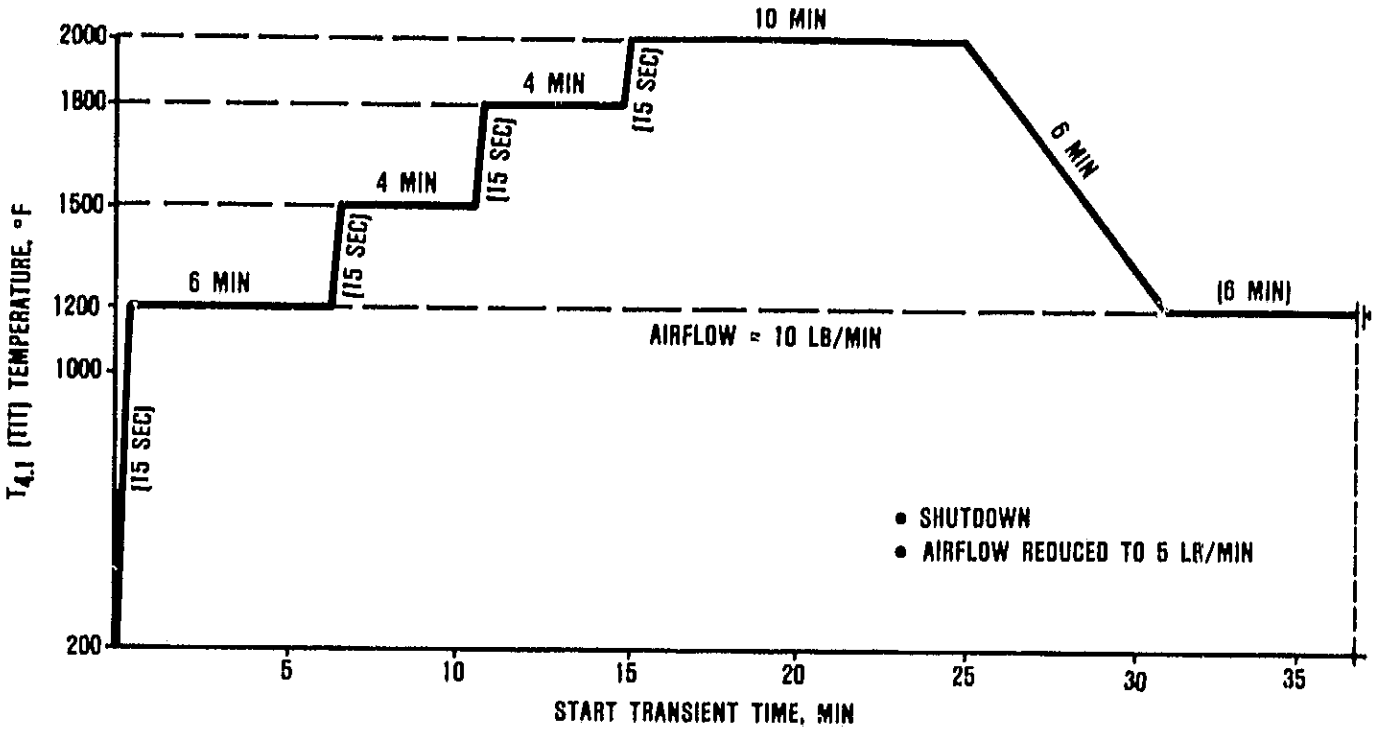

Figure 30. Simulated Development Engine Start Transient.

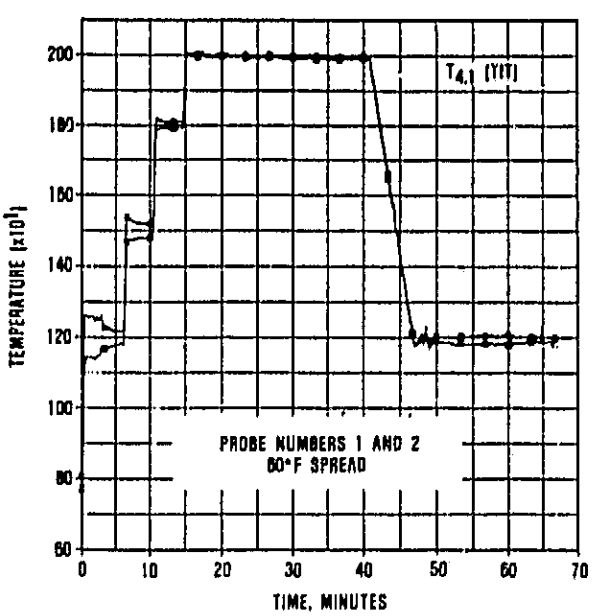

Figure 31. Typical TIT Trace at Idle.

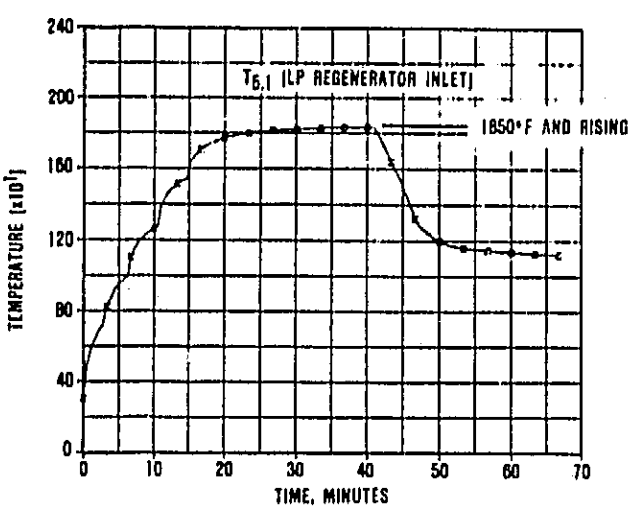

Figure 32. Low Pressure Regenerator Inlet Temperature Versus Cycle Time.

Figure 33. Vacuum Formed Insulation Coating Degradation.

Test Procedure

Build 9

On September 28, 1983 the second complete set of development engine static structural hardware (Table 8) was tested to 2000°F using the identical start transient of Build 8, Figure 30.

At two minutes into the second 2000°F thermal transient the acoustic emission monitor picked up a continuous high energy output from the number three bolt location. The acoustic trace shown in Figure 34 shows the RMS output saturated and a count rate (counts/event) was observed in the 900-1000 range. Due to the high energy indication the test was terminated and the rig disassembled.

A statistic and summary of the test is as follows:

o Total No. of Light-offs	6
o Total time at 1200°F	42 Mins
o Total Time at 1500°F	16 Mins
o Total Time at 1800°F	12 Mins
o Total Time at 2000°F	20 Mins
o Transient Time	20 Mins 15 Sec
o Total Rig Time	1 Hr. 56 Mins

Upon disassembly, component inspection revealed a fractured turbine shroud and a chip from the outer diameter of the outer diffuser near the second bolt location (7 o'clock position). The inner and outer diffuser assembly is spring loaded against the turbine shroud mounting flange through the eccentric spacer at this location. Eccentrics at the second and third bolt locations were lightly "stuck" together in the unloaded position due to apparent foreign material lodged between the eccentric and the rocker during test. This unloaded

TABLE 8. DEVELOPMENT ENGINE STATIC STRUCTURAL HARDWARE

Three Materials, Six Fabrication Processes, Six Suppliers
In B/N(9)

Component Name	S/N	Material	Source	Quantity	Design Configuration
Regenerator Shield	108	SASC	CBO	1	A-1
Regenerator Shield Piston Ring	003, 004	RSSC	Pure Carbon	2	A-1
Flow Separator, Housing	12	LAS	Corning	1	A-2 (3-$T_{4.1}$ Probes)
Regenerator Core		MAS	NGK	1	Coated Thick Wall
Transition Duct	102	SSN	NGK	1	A-3 (3-$T_{4.1}$ Probes)
Transition Duct $T_{4.1}$ Bushing	004, 005, 006	SASC	CBO	3	A-1
$T_{4.1}$ Inner Seal (Female)	004, 005, 006	LAS	Corning	3	A-1
$T_{4.1}$ Inner Seal (Male)	004, 005, 006	LAS	Corning	3	A-3
$T_{4.1}$ Inner Seal Spacer	004, 005, 006	LAS	Corning	3	A-1
$T_{4.1}$ Inner Seal Load Spacer	004, 005, 006	LAS	Corning	3	A-1
$T_{4.1}$ Outer Seal (Female)	004, 005, 007	LAS	Corning	4	A-1
$T_{4.1}$ Outer Seal (Male)	004, 005, 007	LAS	Corning	4	A-1
Combustor Baffle	111	SASC	CBO	1	A-2 (0.200 Wall-Uniform)
Turbine Backshroud	105A	SASC	CBO	1	A-1
Turbine Stators (Seg.)	Set #3	RBSN	ACC	18	A-1
Turbine Shroud	354	RBSN	ACC	1	B-3
Turbine Shroud I.D. Seal	002	RBSN	ACC	1	A-1
Turbine Shroud Wave Spring	002	RBSN	ACC	1	A-1
Turbine Shroud O.D. Seal	LASS 001	RBSN	ACC	1	A-1
Outer Diffuser Housing	297	RBSN	ACC	1	A-3 (Dump Section)
Inner Diffuser Housing	309	RBSN	ACC	1	B-2
Inner Diffuser Load Spacer	004, 005, 006	LAS	Corning	3	A-1
Bolt Assembly	007, 008, 009	HPSN	Norton	3	A-1
Rocker	007, 008, 009	HPSN	Norton	3	A-1
Eccentric	007, 008, 009	HPSN	Norton	3	A-1
Contract Washer (Upper)	007, 008, 009	HPSN	Norton	3	A-2 (0.150 Thickness)
Contract Washer (Lower)	007, 008, 009	HPSN	Norton	3	A-2 (0.150 Thickness)
Crowned Washer	007, 008, 009	HPSN	Norton	3	A-1

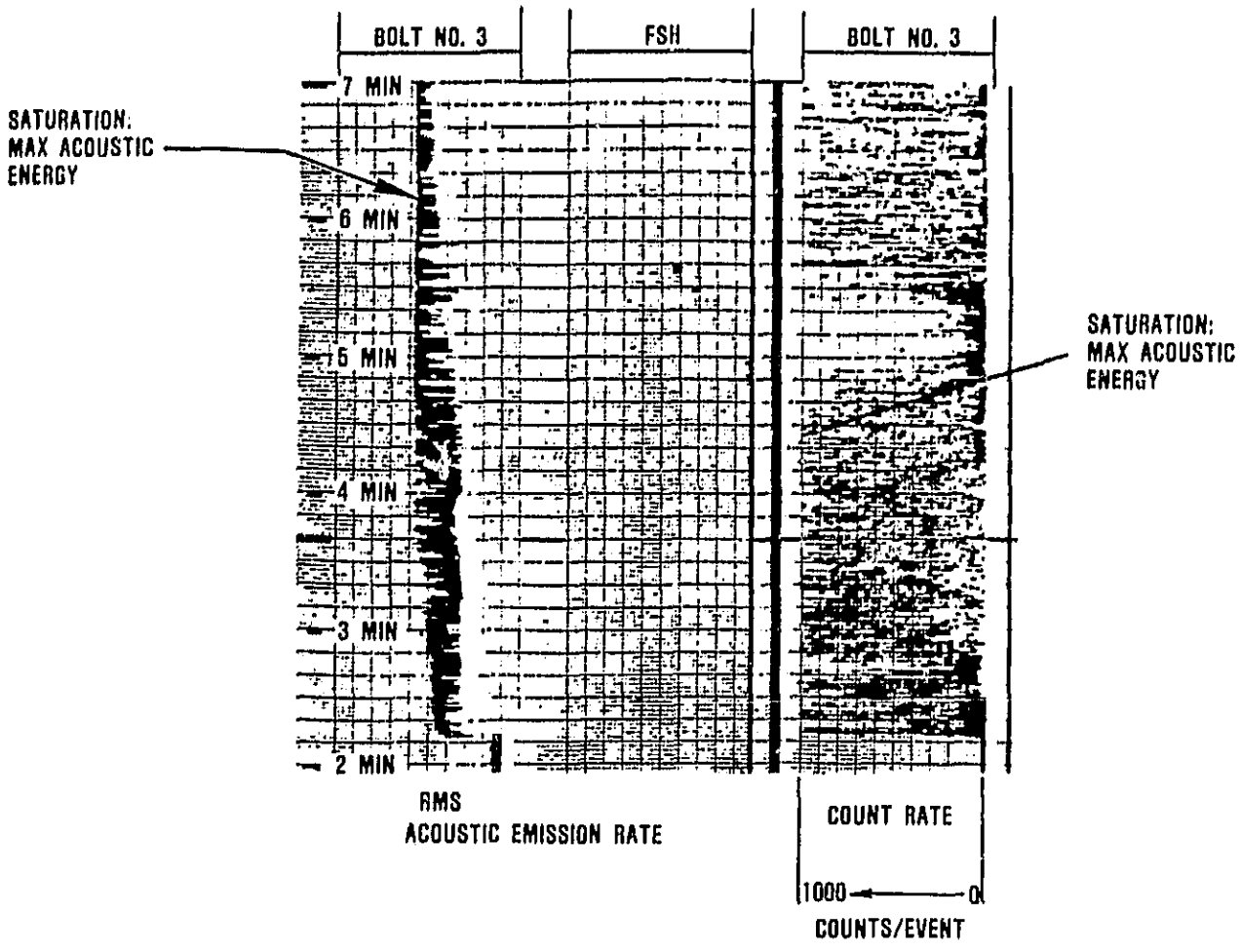

Figure 34. Acoustic Emission Trace, Build 9.

position can allow the outer diffuser to vibrate against the turbine shroud due to recirculating flow behind the outer diffuser with pressure differential from diffuser inlet to discharge as the driver.

Fracture Analysis

The turbine shroud fractured at a surface defect as indicated in Figure 35. The defect was approximately 0.125 inch in depth.

Fracture of the turbine shroud occurred at a time in the cycle when the analytically predicted thermal stress was less than 1 ksi. Since the shroud had survived a higher thermal stress at 1200°F (200 to 1200°F transient) thermal stress was ruled out as the cause of fracture. Further, since the shroud had successfully completed the first cycle to 2000°F without a fracture indication a safe assumption is that no interference was present.

The one outstanding feature of the fracture was the unique acoustic signature, which gave the appearance of high energy vibration between two major components. Since the outer diffuser housing was "loose" in the stack due to the apparent sticking (FOD) at the number two and three bolt locations, a vibration mode could conceivably be exited into the stack by the 10 lb/min airflow, and the pressure differential across the part.

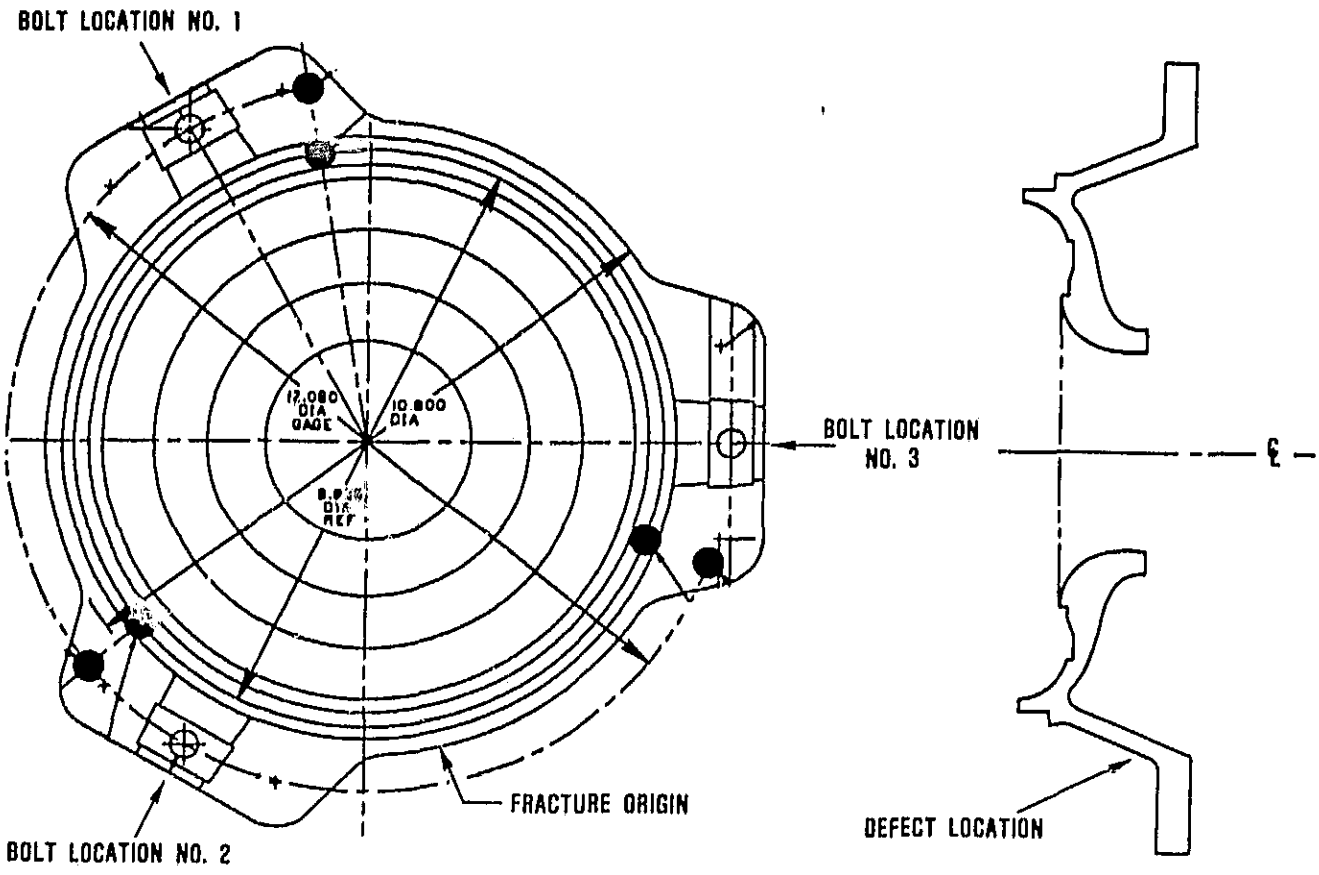

Figure 35. Turbine Shroud Fracture.

On the basis of outer diffuser to turbine shroud vibration a test was conducted on the inner and outer diffuser thermal screening rig in which the ODH was deliberately stacked loose to the turbine shroud (0.010-0.020 inch axial clearance). The acoustic wave guide was installed on the number three bolt and the ODH was manually vibrated against the turbine shroud mounting flange. Figure 36 shows the acoustic response from this test and indicates a signature comparable with Build 9 but with an expected lower energy level (RMS and Count Rate).

Garrett believes that the vibratory energy from the ODH to the turbine shroud in Build 9 contained sufficient energy to propagate the existing surface defect and chip the diffuser OD at the point closest to bottom dead center.

Recommendation

To preclude the potential of this problem the spring load across the inner/outer diffuser housing stack has been increased from 21 lb_f to 80 lb_f.

Build 10/10A

During Build 10 assembly the compressor backshroud was replaced with updated dimensional hardware. The new hardware was installed and a leak check performed, and excessive leakage was noted. Upon disassembly, it was noted that the axial stack between the shroud/flow separator housing (FSH) seal

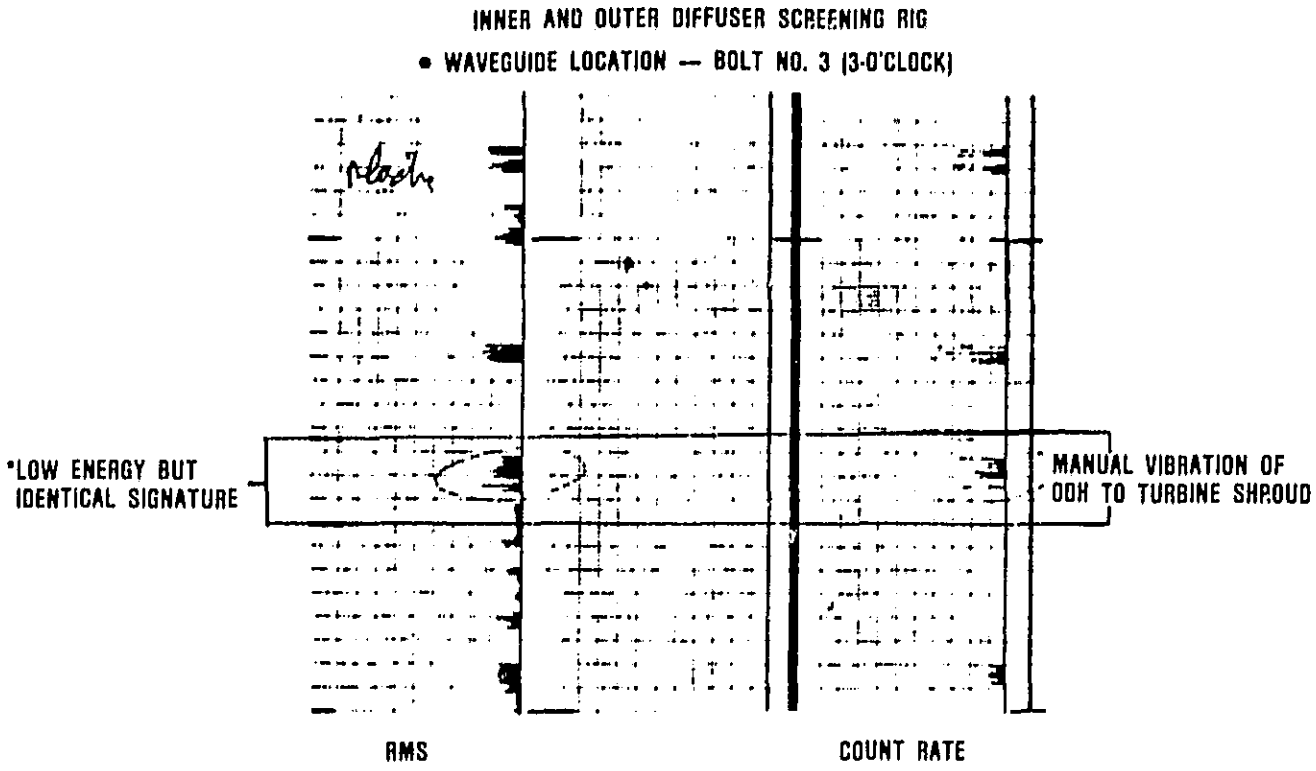

Figure 36. Simulated Vibration Test for Outer Diffuser Housing to Shroud.

platform resulted in a GAP, thus allowing HP-to-LP communication. As shown in Figure 37, 0.050 inch was removed from the FSH to effect sealing. This unit was reassembled and testing initiated.

On October 10, 1983, the AGT101 Ceramic Static Structures Rig successfully qualified all but one of a complete development engine assembly of ceramic static structural components (Table 9) through ten (10) simulated engine start transients to 2000°F. A statistical summary of the test is as follows:

o	Total Light-Offs	12
o	Time at 1200°F	1 Hr 40 Min
o	Time at 1500°F	40 Min
o	Time 1800°F	40 Min
o	Time at 2000°F	1 Hr 40 Min
o	Total Rig Time	5 Hrs 50 Min

At 19 minutes, 20 seconds into the first transient cycle (2000°F) a 91 db event was recorded on the FSH acoustic emission monitor. The count rate for the event was approximately 450 counts indicated a probability of fracture. However, no changes were noted in rig HP or LP inlet pressures, and there was no fluctuation in regenerator drive torque following the event, therefore, the test was continued.

Air-cooled Phase IV regenerator seal testing was continued in Build 10 with increased air passage relief to accommodate higher cooling airflow. The modified cooling passages had no positive effect on either the metallic diaphragm or substrate temperature over the previous configuration of Build 9. A new cooled seal Configuration V is being pursued by Ford (Phase V). The test was concluded following the successful completion of 10 simulated development engine start transients to 2000°F.

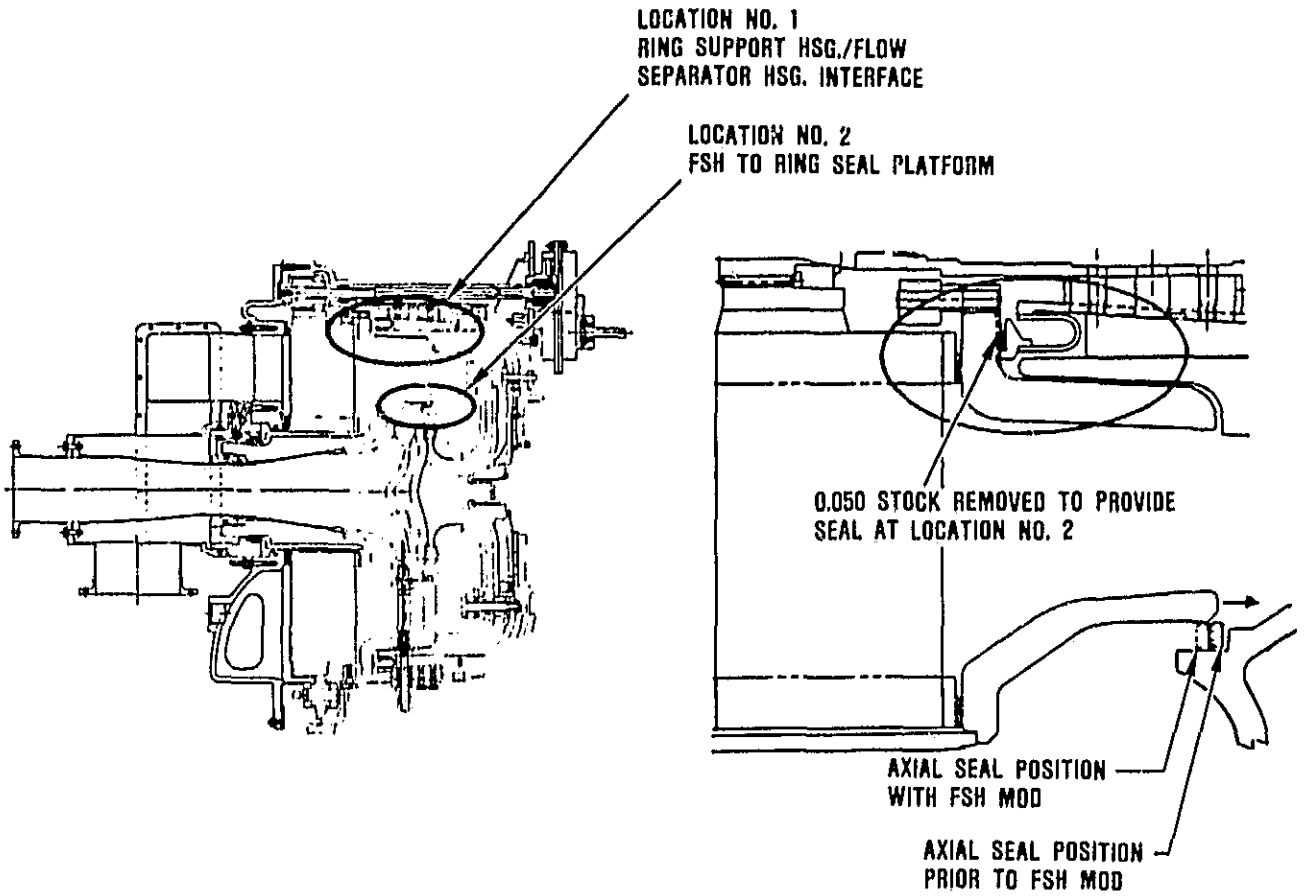

Figure 37. Stock Removed From Flow Separator Housing Platform to Provide Axial Seal.

At disassembly it was noted that the inner diffuser housing had fractured during test and the flow separator housing had an axial crack along the LP flowpath wall at the 10-11 o'clock position. The FSH fracture occurred at the time indicated by the acoustic monitor.

FRACTURE ANALYSIS

Inner Diffuser Housing

Fracture of the inner Diffuser Housing (IDH) originated at the number 1 and number 2 bolt locations as illustrated in Figure 38. Apparently, from investigation of the insulation, the IDH was forced against the indicated bolt locations by a reactive load on the pilot diameter of the insulation preform as the IDH thermally expanded. Inadequate diametral clearance between the IDH and the insulation preform (in its coated and hardened condition) has been determined the primary cause of the fracture. With the IDH forced against the numbers 1 and 2 bolt locations, the acoustic emission probe (located on bolt number 3) had no direct sound path to the IDH and no fracture signature was recorded.

Flow Separator Housing

Figure 37 illustrates the undercut required in the FSH mounting platform to provide axial sealing with the turbine shroud. During operation, a radial interference between the ring support housing and the FSH mounting platform developed, as the unit was heated to 2000°F, resulting in fracture in the undercut

TABLE 9. DEVELOPMENT ENGINE STATIC STRUCTURAL HARDWARE

Three Materials, Six Fabrication Processes, Six Suppliers
In B/N(10)

Component Name	S/N	Material	Source	Quantity	Design Configuration
Regenerator Shield	108	SASC	CBO	1	A-1
Regenerator Shield Piston Ring	003, 004	RSSC	Pure Carbon	2	A-1
Flow Separator, Housing	12	LAS	Corning	1	A-2 (3-$T_{4.1}$ Probes)
Regenerator Core		MAS	NGK	1	Coated Thick Wall
Transition Duct	102	SSN	NGK	1	A-3 (3-$T_{4.1}$ Probes)
Transition Duct $T_{4.1}$ Bushing	004, 005, 006	SASC	CBO	3	A-1
$T_{4.1}$ Inner Seal (Female)	004, 005, 006	LAS	Corning	3	A-1
$T_{4.1}$ Inner Seal (Male)	004, 005, 006	LAS	Corning	3	A-3
$T_{4.1}$ Inner Seal Spacer	004, 005, 006	LAS	Corning	3	A-1
$T_{4.1}$ Inner Seal Load Spacer	004, 005, 006	LAS	Corning	3	A-1
$T_{4.1}$ Outer Seal (Female)	004, 005, 007	LAS	Corning	4	A-1
$T_{4.1}$ Outer Seal (Male)	004, 005, 007	LAS	Corning	4	A-1
Combustor Baffle	111	SASC	CBO	1	A-2 (0.200 Wall-Uniform)
Turbine Backshroud	105A	SASC	CBO	1	A-1
Turbine Stators (Seg.)	Set #3	RBSN	ACC	19	A-1
Turbine Shroud	354	RBSN	ACC	1	B-3
Turbine Shroud I.D. Seal	002	RBSN	ACC	1	A-1
Turbine Shroud Wave Spring	002	RBSN	ACC	1	A-1
Turbine Shroud O.D. Seal	LASS 001	RBSN	ACC	1	A-1
Outer Diffuser Housing	297	RBSN	ACC	1	A-3 (Dump Section)
Inner Diffuser Housing	309	RBSN	ACC	1	B-2
Inner Diffuser Load Spacer	004, 005, 006	LAS	Corning	3	A-1
Bolt Assembly	007, 008, 009	HPSN	Norton	3	A-1
Rocker	007, 008, 009	HPSN	Norton	3	A-1
Eccentric	007, 008, 009	HPSN	Norton	3	A-1
Contract Washer (Upper)	007, 008, 009	HPSN	Norton	3	A-2 (0.150 Thickness)
Contract Washer (Lower)	007, 008, 009	HPSN	Norton	3	A-2 (0.150 Thickness)
Crowned Washer	007, 008, 009	HPSN	Norton	3	A-1

fillet region. No secondary damage to either the FSH or the regenerator core was observed.

4.5.4 Ceramic Turbine Rotors

4.5.4.1 Ceramic Material Development

ACC continues to fabricate rotors of 8-percent Y_2O_3, 4-percent Al_2O_3 compositions. Rotors are cast, dried, and presintered by ACC; Ford continues to sinter rotors to final density. Sintering experiments have continued at ACC and ASEA, and ACC continued to improve rotor surface quality and yield. Efforts also continued on controlled temperature/humidity drying of the rotors to eliminate blade angle cracks.

During this period Ford sintered four rotors to densities in excess of 98.8 percent theoretical. Three of these rotors have passed non-destructive evaluation (NDE) inspection. Two rotors (S/Ns 426 and 472)are presently being machined for spin testing. The third rotor (S/N 316) exhibited surface cracks and was cut into test bars for evaluation. The fourth rotor (S/N 353) is being NDE inspected.

ACC sintered three rotors. Two rotors sintered at 3272°F/100 psi N_2 achieved densities of 96.6 percent theoretical. NDE inspection indicated internal defects in those rotors verified by destructive (cut-up) evaluation. One of these rotors (S/N 431) is being used to verify and possibly calibrate the ultrasonic NDE technique.

One rotor sintered at 3362°F/15 ksi N_2 achieved a density of 98.5 theoretical and passed NDE inspection. This rotor (S/N 542) is being machined for spin testing.

During this period three rotors and several test specimens were furnished to ASEA-

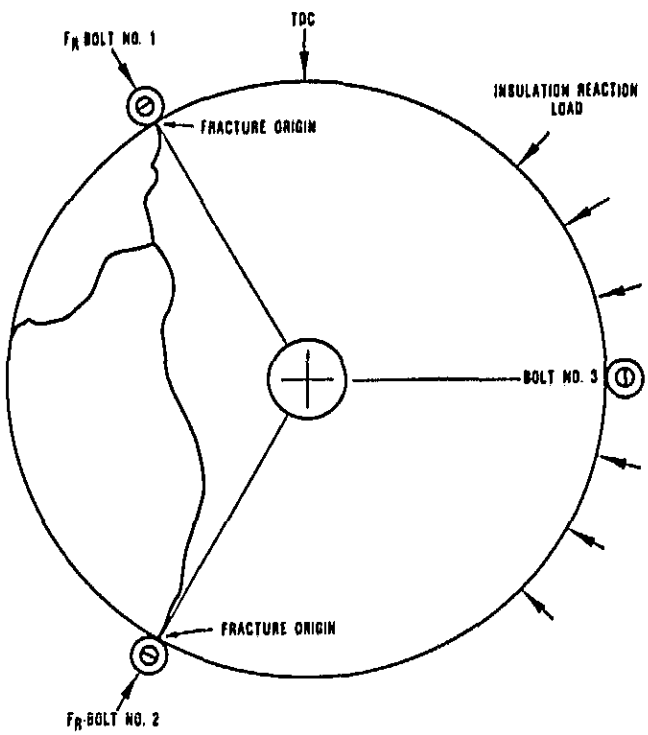

Figure 38. Inner Diffuser Housing Fracture (Structures Rig Build 10).

Sweden for glass encapsulated HIP experiments. Based on the test specimen experiments three rotors were HIP processed at 3002°F/30 ksi achieving densities of 95-99 percent theoretical. These rotors were not considered good quality and did not incorporate the latest ACC casting technology but served the purpose of evaluating ASEA's densification technique. One rotor (S/N 565), which passed visual (10-40x) inspection, was NDE inspected and passed. This rotor is being machined for spin testing. Table 10 presents the status of ACC rotors received by Garrett.

The flexure strength of test bars cut from two fully processed rotors were determined. The results are presented in Table 11.

4.6 Rotor Dynamic/Foil Bearing Development

Effort continued on rotor dynamics development in support of resolving the subsynchronous motion noted during engine testing. Activities have included screening foil bearings for engine test, evaluating shaft dampers and initiating a thorough thermal mapping of the test rig environment and engine environment. In addition, alternate bearing configurations are being investigated on an active basis.

4.6.1 Rotor Dynamic Rig Testing

A brush seal was designed and fabricated for use as a shaft damper in the vicinity of the foil bearing. Initial testing showed favorable results in limiting subsynchronous and synchronous motion of the rotating assembly. Two variations (0.010 and 0.020 inch diametral interference) design were evaluated along with two shaft coating systems. Figure 39 shows the brush seal installation.

Initial testing in the rotor dynamics rig showed improvement in suppression of the synchronous and subsynchronous motion. However, frictional heat generation and debris was noted. A design modification was incorporated to add additional cooling benefits to the journal region and actively remove the debris. However, as previously stated in Section 3.2, the brush seal does not appear viable as a long term solution. Table 12 shows power consumption test results for the configutation evaluated.

4.6.2 Analysis

The foil bearing/journal environment has been analytically modeled using assumed boundary conditions. Results of this analysis indicated a well exhausted system thermally, however numerous bearing configurations run stably in the test rig while performing poorly in the engine. A major difference between the rig and engine is the thermal environment, therefore, installation of thermocouples (TCs) directly on the foil leaves was undertaken. Figures 40 through 43 depict the location and number of TCs requested. This effort was underway at the close of the reporting period, and results will be forthcoming.

TABLE 10. CERAMIC ROTORS RECEIVED FROM ACC

JULY 1 - DECEMBER 31, 1983

Rotor	Process Status	Comment
S/N 316	Sintered/passed NDE	Cut up for test bars
S/N 426	Sintered/passed NDE	Being machined for spin test
S/N 378	Sintered/failed NDE	Cut up for test bar
S/N 431	Sintered/failed NDE	Cut up for NDE verification
S/N 472	Sintered/passed NDE	Being machiend for spin test
S/N 565	Sintered/passed NDE	Being machined for spin test
S/N 542	Sintered/passed NDE	Being machined for spin test
S/N 552	Sintered	Being NDE inspected
S/N 562	Presintered	At Ford for sintering
S/N 563	Presintered	At Ford for sintering
S/N 564	Presintered	At Ford for sintering

TABLE 11. FLEXURE STRENGTH OF TEST BARS CUT FROM FULLY PROCESSED ACC ROTORS AT ROOM TEMPERATURE AND 2200°F

Rotor	Density Sintered by	% Theoretical	Flexural Strength[1, 2]					
			Room Temperature			2200°F		
			θ	m	N	θ	m	N
S/N 316	Ford	98.8	113	16.6	20	54	9.5	10
S/N 378[3]	ACC	96.7	95	7.5	20	51	6.6	10

[1] 1/4 point bend, 1.50-inch outer span, 0.125 x 0.250 x 2 inch-specimen

[2] θ = Characteristic strength, m = Weibul slope, N = sample size

[3] Rotor S/N 378 contained pores detected by NDE which were the fracture origins

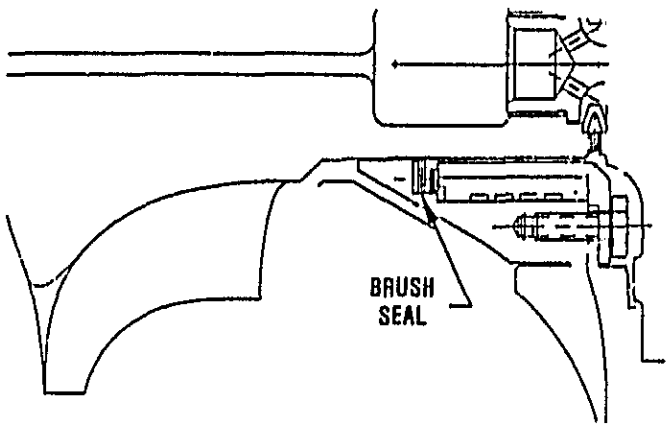

Figure 39. Brush Seal Installation.

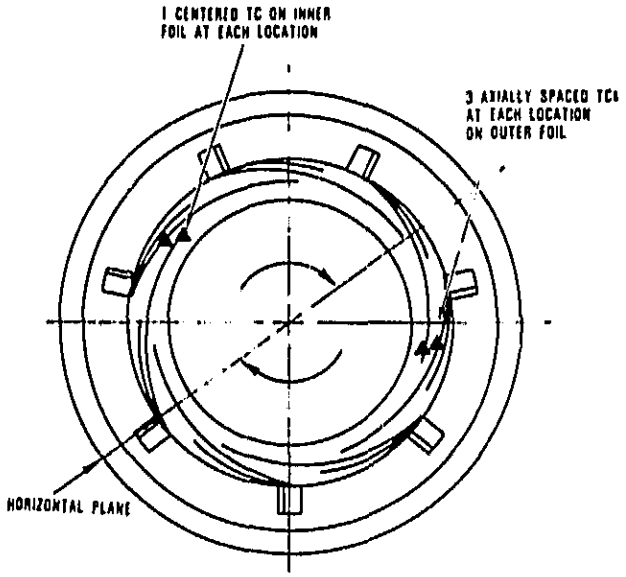

Figure 40. AGT Foil TC Locations.

4.6.3 Alternate Bearing Systems

Due to the technical problems encountered in resolving rotor stability, two alternate systems are being pursued; Hydrodynamic Oil Film Thrust Bearing, and Pivoted Pad Air Bearing. The alternates address similiar but different areas of the instability question.

A fluid film oil thrust bearing can be added to the compressor end or the shafting inboard of the existing ball bearing. An analytical study was conducted to ascertain the possibilities of achieving significant radial and torsional dampening using the hydrodynamic bearing. Results of this study were positive and detail design and fabrication was initiated.

The concept involves the utilization of a circular thrust runner on the engine shaft inboard of the existing ball bearing. The runner is straddled by two oil lubricated thrust washers that are supported by carriers fixed to the housing. The ball bearing outer race is retained in a hydraulic mount and is unrestrained axially except for a 10- to 50-pound axial pre-load to prevent skidding.

Figure 44 (top half) illustrates a cross section through the thrust and radial bearings

TABLE 12. SUMMARY OF BRUSH SEAL STEADY-STEADY POWER CONSUMPTION AT MAXIMUM SPEED (100,000 RPM)

Shaft Coating	Brush Seal Power Consumption, Watts			
	0.010 Inch Interference	0.020 Inch Interference	25% Slot Cutaway	50% Slot Cutaway
SCA:				
Cooled	315	423	102	163
Uncooled	314	456	150	166
METCO 105:				
Cooled	161	343	NOT	184
Uncooled	268	311	RUN	225

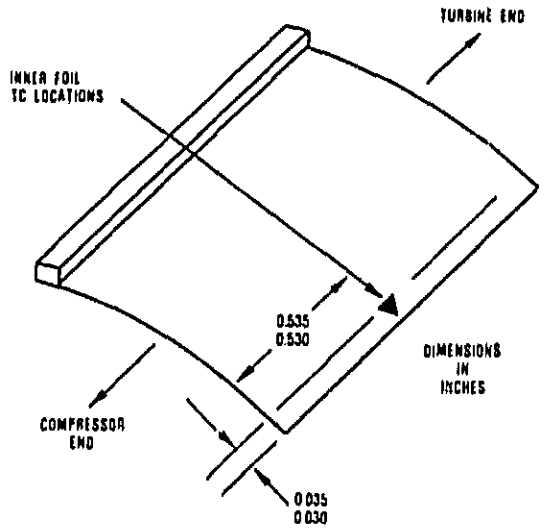

Figure 41. AGT Inner Foil TC Locations.

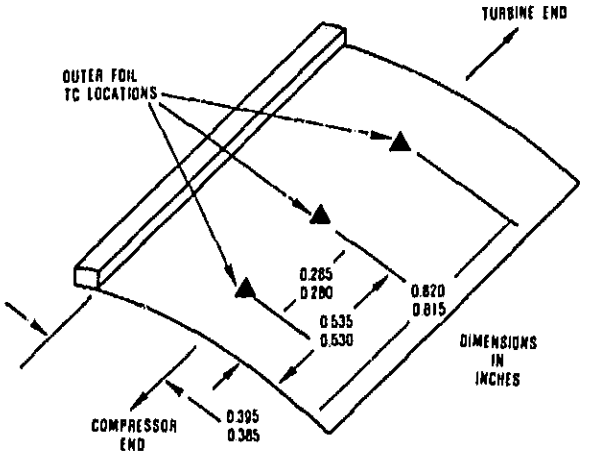

Figure 42. AGT Outer Foil TC Locations.

of the AGT101 engine in the baseline configuration. Note that the engine net thrust is transmitted to the housing through the ball bearing.

Figure 44 (bottom half) illustrates a cross section through the same part of the engine when modified to accommodate the hydrodynamic thrust bearing in conjunction with the ball radial bearing.

Proper alignment of the thrust washer with the thrust rotor at initial assembly is crucial to proper bearing operation. To assure proper alignment, the interface seat surfaces of the washer and the thrust plate assembly are made spherical with the center of the spherical radius at the intersection of the engine shaft centerline and a radial plate through the axial center of the foil bearing. This configuration will permit the thrust washer to align exactly flush with the mating thrust surface of the thrust rotor. This arrangement also will sustain this alignment through small displacements of the housing or the shaft during thermal excursions in engine operation.

The second alternate is a pivoted pad air bearing. The design heavily draws from the successful Garrett Brayton Rotating Unit (NASA CR-1870). Benefits of the pivoted pad design include additional stiffness to the rotating system as well as damping. A summary of salient bearing features is presented below:

Journal diameter - 1.66 inches
Number of pads - 3
Pad effective arc length - 100 degrees
Pad width - 0.703 inch

Figure 45 shows this bearing installed in the engine and a sectional view is depicted in Figure 46.

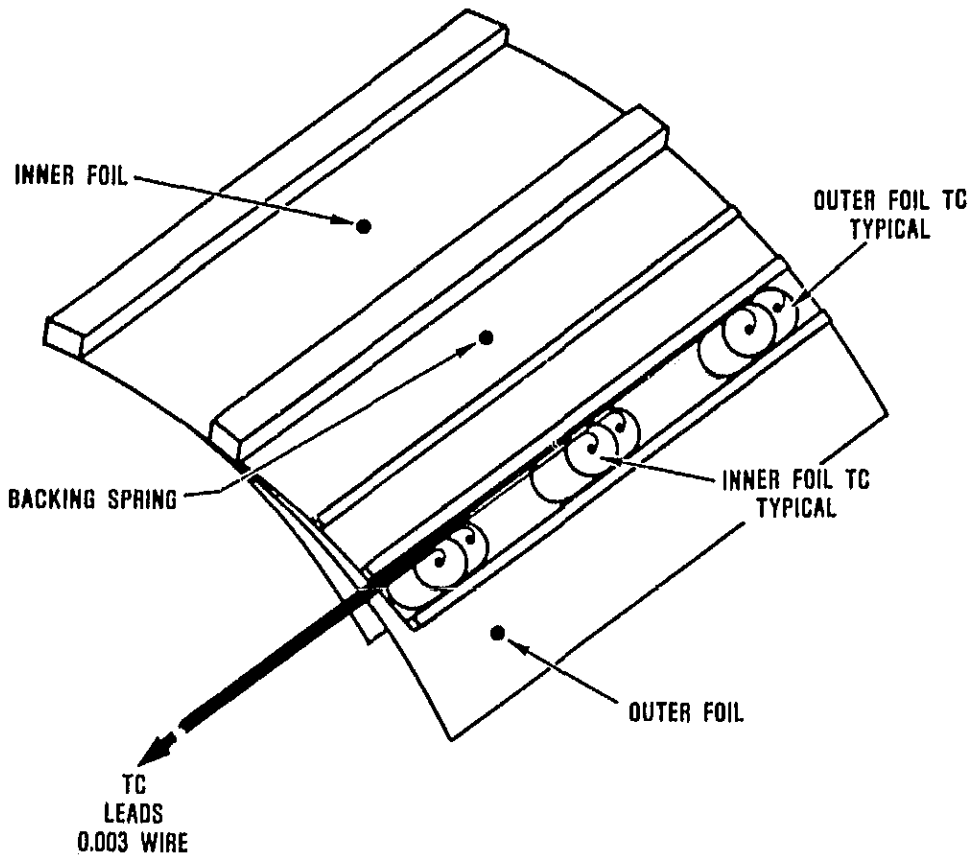

Figure 43. Foil Instrumentation.

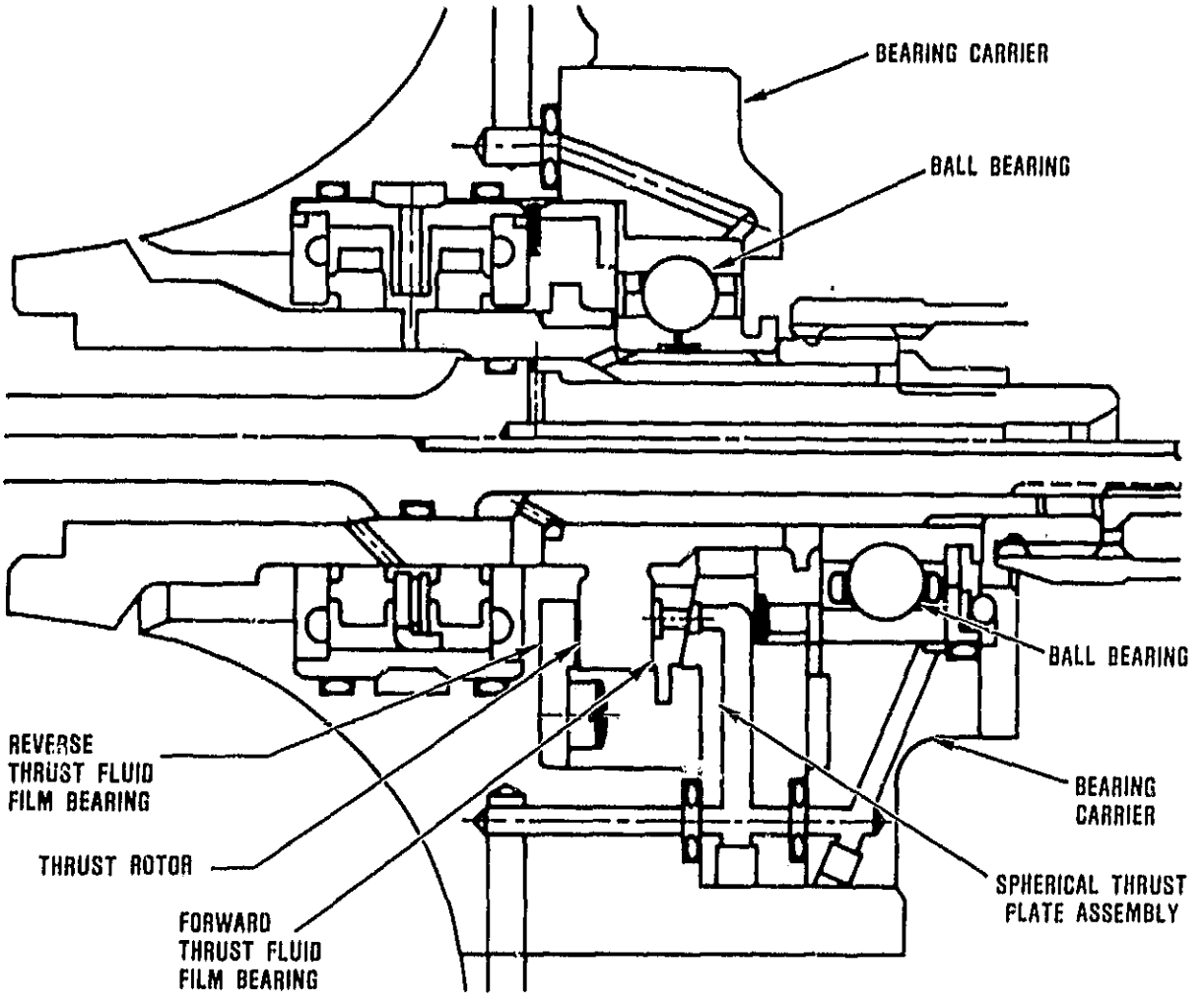

Figure 44. Hydrodynamic Fluid Film Thrust Bearing Installation.

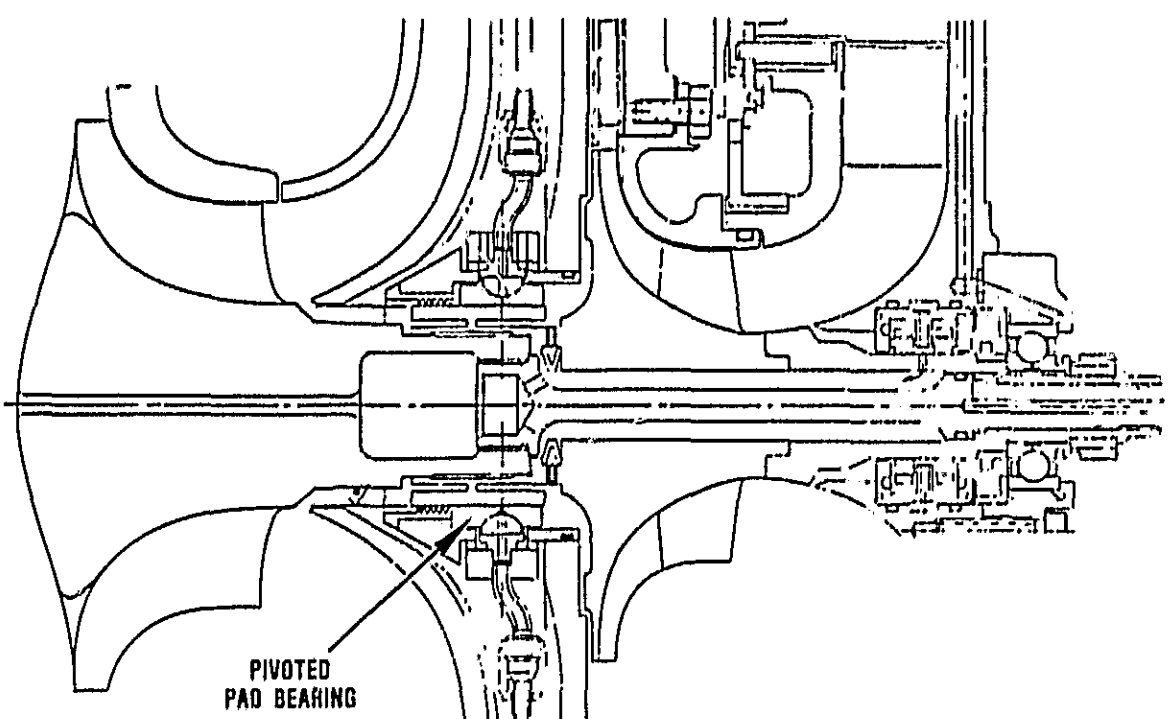

Figure 45. Pivoted Pad Air Bearing Installed in Engine.

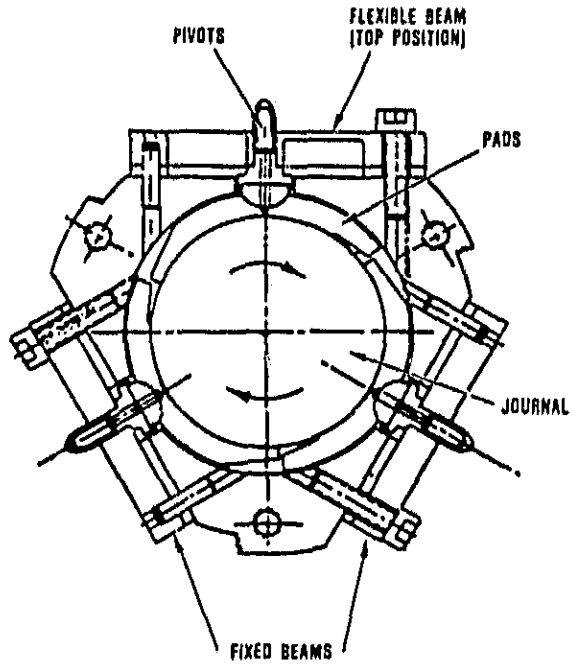

Figure 46. Pivoted Pad Bearing - Additional Features.

APPENDIX A

FORD MOTOR COMPANY
ADVANCED GAS TURBINE (AGT) POWERTRAIN
SYSTEM DEVELOPMENT PROGRAM
EIGHTH AGT101 SEMI-ANNUAL
TECHNICAL PROGRESS REPORT

1. TASK 2.3 - CERAMIC ROTOR

1.1 Material Development and Characterization

Testing of RM-3, reported in the seventh semi-annual report, showed that this material exhibits good oxidation behavior in the 1832°F region as well as good stress rupture behavior up to 50 ksi at 1832 and 2192°F. Testing conducted this period identified a stress rupture problem for stress levels beyond 50 ksi at both 1832 and 2192°F. The results show that the samples will either fail in less than 8 hours or survive without failure for over 100 hours. Preliminary analysis indicates that premature failure may be related to a non-uniform flash oxidation on the test samples. Work is continuing to improve the uniformity of the oxidation treatment.

Despite these inconsistent results at high stress levels, the RM-3 SRBSN was shown to exceed the stress rupture requirement of 30 ksi at 2050°F. However, in an effort to provide longer term material capability, development of material improvements has been initiated. Several modified compositions will be investigated and evaluated for oxidation and stress rupture behavior. The effort will concentrate on modifications that produce an inherent oxidation protection mechanism rather than relying on flash oxidation.

Work to understand the fracture mechanisms in RM-2 material also is progressing. Results to date indicate that non-uniformities in microstructure are the principal cause of room temperature failure. The results of this study will be incorporated in the work on improved material development.

1.2 Bladed Rotor Fabrication

As noted in the seventh semi-annual report, basic investigations were completed in characterizing slip properties and slip behavior and models were formulated to predict slip performance. Slips with a polymer addition have improved the quality of cast rotors.

The slip condition is controlled by test bar density. A study to correlated nitrided densities of test bars and rotors, cast from the same slip, was completed and results are shown in Figure 47. As shown in the figure, test bars achieve a higher density than rotors when made from the same slip. This relationship determines the characteristics of the slip required to obtain rotors of the desired density. Also noticed was that the ratio of the volume of the plaster mold to the mold surface area influences the green density of test bars. Data given in Figure 48 show how the green density is influenced by both the viscosity of the slip and the volume-to-area ratio of plaster in the mold. These correlations of properties of test bars and nitrided rotors are necessary because the fragile condition of the as-cast rotors precludes density measurements.

Sixteen rotors were cast during this period with slips containing improved properties. Twenty rotors were nitrided with some blade and hub cracking in each. Four serial numbers, V-5, 6, 8, 9, were sintered with the best rotor (V-9) having a density of 3.21 g/cm^3. These rotors all have too low a density for testing.

As indicated in the seventh semi-annual report, the new technique for removal of wax

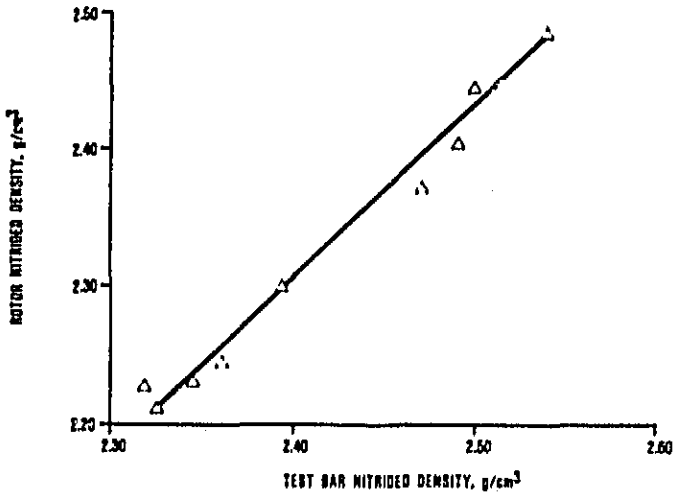

Figure 47. Rotor Vs Test Bar Density.

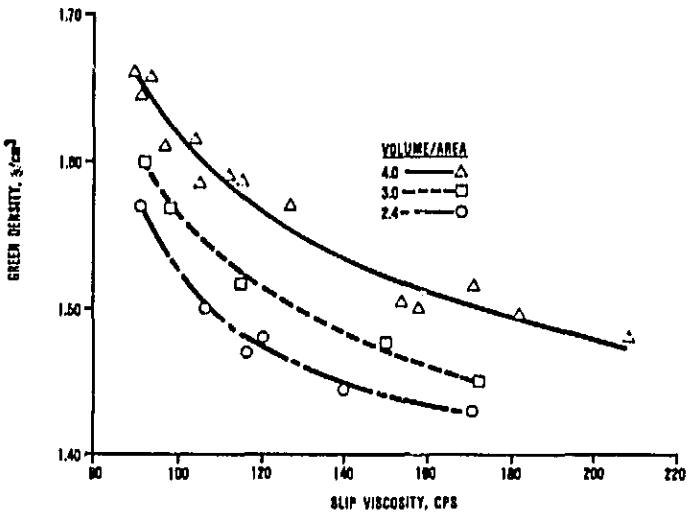

Figure 48. Green Density Vs Slip Viscosity.

from the fragile slip cast rotor continues to provide cast rotors with improved quality. The technique has been refined to the point where there are no visible flaws evident in the green casting, and when present, the flaws are visible only after nitriding.

Work continued during this reporting period on the slip casting of rotors using a modified SRBSN material, designated RM-20. Slip casting techniques investigated used the was mold process to produce bladed rotors for spin evaluation. The effect of powder sizing, flocculating agents, and mold modifications are being evaluated. Two rotors have been successfully cast and sintered to 3.24 g/cm^3 density and appear to be of high quality (S/Ns SC-1, SC-8). Rotor S/N SC-1 produced by this process was spin tested and failed at 77,700 rpm. The origin of failure was a large spherical porosity in the hub. Rotor S/N SC-8 will be proof tested in the spin pit in the next reporting period. Six additional rotors have been slip cast and await sintering.

Design of the 'B' configuration rotor injection molding tooling was completed this report period. The belief is that the new design will improve changes for successful fabrication. This tooling is on order and will be delivered in April, 1984.

Three slip cast and nitrided SRBSN rotors, S/Ns 140, 146, and 149, were sent to ASEA to be hot isostatic pressed (HIP) in an attempt to increase density to theoretical and to heal apparent cracks in hub and blades. The rotors have been returned, and S/N 140 has been spun in the cold spin pit. Failure occurred at 72,000 rpm. S/N 146 will be tested in the spin pit and the third rotor sectioned for observation of success in crack healing.

2. TASK 2.7 - STATOR

2.1 Molded Stator Processing

Longer range plans were made to investigate SRBSN integral stators, as noted in the seventh semi-annual report, to utilize improved properties of SRBSN for increased stator reliability. Of the twenty-two stators molded with a SRBSN mix, one completed the burn-out, nitriding and sintering cycles. However, the stator was badly distorted after sintering. Sectioning of the stator revealed that the layering of the molding material occurred during injection molding. Distortion

during sintering was caused by separation of the material layers, which produced large voids. Additional stators will be processed to determine the extent of this condition.

Discussions with Garrett indicate that a stator assembled from two half sections of the integral stator would be useful. Several of the 2.7 g/cm^3 stators previously molded are crack-free in a one-half section of the stator, and these are being processed through the burn-out and nitriding cycles. Two stators shipped to Garrett for evaluation, S/Ns 1209206 and 1208205, await testing in the stator thermal screening rig. These stators contain small, tight cracks in several vane fillet radii in both leading and trailing edges on the shroud segmented side.

2.2 Fillet Crack Investigation

As discussed in the seventh semi-annual report, a systematic study was conducted to establish a relationship between molding variables and the extent of fillet cracks. During this reporting period, a series of stators were molded to investigate the four variables previously identified as significant to creation of leading and trailing edge cracks and fillet cracks found in previous stators.

Several conclusions were obtained from these studies. The cracks were molding related and could be seen in green stators immediately after molding. For the same injection molding cycle settings and sequence items, similar crack patterns were produced. The leading edge cracks were closely related to the gate region and also related to gate relocation. Both the leading and trailing edge cracks were reduced by changing to a tapered sprue, longer time to open the die, and reduced injection pressure.

These studies were made using a 0.015 x 3 inch gate. Although the results showed promise in eliminating the fillet cracks, shroud cracks and shroud tear-out in the gate area occurred. These problems were attributed to sticking of the molded part to the tool cavity from localized overheating. Increasing the gate size to 0.065 x 3 inches eliminated the overheating problem. Molding conditions were identified that yield 50 percent or more stators, which are free of trailing edge and leading edge cracks. Other molding conditions were identified that yield 80 percent of the stators with crack-free tailing edges. Molding development is continuing toward producing stators without trailing edge cracks.

During this report period, an automatic sequencer was installed on the Temperaft vertical molding machine and programmed for the AGT stator. The sequencer has demonstrated excellent repeatability of the molding cycle time events.

3. TASK 2.7 - FLOW SEPARATOR HOUSING

While no fabrication or development work was scheduled for this reporting period, a purchase order for five components was placed with Corning.

APPENDIX B

AIRESEARCH CASTING COMPANY (ACC) ADVANCED GAS TURBINE (AGT) POWERTRAIN SYSTEM 101 DEVELOPMENT PROGRAM EIGHTH AGT101 SEMI-ANNUAL TECHNICAL PROGRESS REPORT

1. SUMMARY

Spin testing of rotor S/N 344, fabricated and densified at ACC, was successfully accomplished to 115,000 rpm, qualifying this rotor for hot turbine rig testing. Rotor fabrication efforts have continued with improved appearance and yield.

Effort is progressing on Code 2 rotor fabrication (6-percent Y_2O_3 and 2-percent AL_2O_3).

Fabrication of structural components continued with activity on all components. ACC has accepted green machining of the inner and outer diffuser housings. This effort was initiated during this reporting period. No ACC machined components were delivered. Table 13 is a summary of delivered components during this period.

2. ROTOR-MATERIALS AND FABRICATION DEVELOPMENT

Rotor S/N 344 successfully passed the 115,000 rpm cold spin test. This rotor was fabricated and densified by ACC. Densification to 98.5 percent theoretical (3.26 g/cm^3) was accomplished in the ACC sintering furnace. The rotor then was shipped to Garrett for NDE and machining. Following final grind, this rotor was balanced and successfully cold spun to 115,000 rpm without incident.

A more controlled systematic processing program is now being conducted to improve effort. As noted in reference 7, elimination of the quality and yield of the rotor fabrication to the calcining process, continued investigation of optimum deflocculants, and wax mold removal techniques, have resulted in improvement in visual quality of the castings. Further evidence is noted in the number of rotors delivered to Garrett for evaluation and final processing. These and other processing related steps are being reviewed.

The partial densification/presinter (reference 7) does not affect final densification and will be used for shipping rotors from this point forward. Also, presintering will be utilized on inhouse processed rotors to improve handling and for inprocess visual inspection.

3. CERAMIC STRUCURES

ACC, in cooperation with the machining personnel and engineering staff at GTEC, has been expanding its green machining capabilities. During this reporting period ACC personnel have visited Garrett to learn the techniques used to machine AGT static RBSN components in the green condition. Subsequently, green machining responsibilities have been systematically transferred from Garrett to ACC.

Green machining operations at ACC were initiated on the inner and outer diffuser components due to simplicity and the relatively stable development status, i.e., no shape changes anticipated. Machining fixtures required for this activity were transferred from Garrett to ACC. The success of this initial machining transfer was followed by a transfer of green machining responsibilities for the turbine shroud and, finally, all other ACC cast RBSN parts.

TABLE 13. SUMMARY OF HARDWARE ACC DELIVERED

June 1, 1983 - December 31, 1983

Component	Total Parts Shipped	S/Ns
Bladed Rotor	12	0412302, 316, 344, 378, 426, 431 472, 542, 552, 562, 563, 564
Inner Diffuser	10	294, 298, 299, 309, 311, 317, 318, 337, 348, 366
Outer Diffuser	10	289, 296, 297, 300, 339, 340, 342, 356, 364, 365
Turbine Shroud	27	307, 308, 346, 353, 354, 368, 374, 377 379, 429, 430, 432, 463, 464, 465, 466, 467, 468, 471, 543, 544, 545, 546, 547, 548, 549, 550
Transition Duct	1	210
Turbine Shroud Seal Ring	9	320, 321, 322, 323, 324, 358, 359, 360, 361
Turbine Shroud Seal Spring	12	246, 250, 259, 260, 261, 262, 263, 264, 265, 266, 267, 268
Stator Segments	43	Set 004 - S/Ns 222 - 236 Set 005 - S/Ns 433 - 462

APPENDIX C

THE CARBORUNDUM COMPANY
(UNIQUE WORK)
ADVANCED GAS TURBINE (AGT)
POWERTRAIN SYSTEM DEVELOPMENT PROGRAM
EIGHTH AGT101 SEMI-ANNUAL
TECHNICAL PROGRESS REPORT

1. BACKGROUND

This report summarizes the work carried out on static structures during the time period July 1, 1983 through December 31, 1983. Carborundum continued to work on six different SASC components. Two advanced forming methods, plastic extrusion and plastic forming, were employed in addition to the already proven techniques of injection molding, slip casting, and isopressing/green machining. Both ceramic forming techniques were introduced to the AGT101 program after being successfully developed for fabricating parts of different shapes with similar compositions.

Plastic forming was introduced for the fabrication of combustor baffles which had been made by slip casting and subsequent green machining of the internal profile to obtain an essentially constant wall thickness. The new method was chosen with the goal of improving net shape forming capabilities and eliminating green machining. Plastic extrusion has been chosen as a fabrication method for combustor liners and regenerator shields which so far had been supplied using isopressing/green machining and final grinding. The change to this fabrication technique reflects the overall goal of employing fabrication methods that have high volume, low cost potential. Individual stator segments and turbine shrouds were made by injection molding as in previous years. Isopressing/green machining remained the fabrication process for the transition duct.

2.0 SUMMARY

During this reporting period Carborundum supplied seven as-fired combustor baffles made by slip casting and green machining, two sets of as-fired stator segments, four machined transition ducts and one ground regenerator shield made by isopressing and green machining. Combustor baffles, transition ducts and regenerator shields have repeatedly performed well in various rig tests at Garrett. Because of these successes on combustor baffles the same bimodal ratio was chosen for the plastic forming composition as far as for the casting slip. The feeling was that the 85-90 percent of theoretical density contributed positively to the combustor baffle performance in the severe thermal shock conditions of a 2100°F rig test.

3.0 STATIC STRUCTURES

3.1 Turbine Stator

Individual SASC stator segments were made by injection molding. A new improved injection molding compound with a different plastic system and a somewhat higher plastic content was used to make stator segments in the mold designed for the previously employed system. The new compound (B) is superior to the old one (A) by producing parts with less molding defects or flow lines. Parts made of compound B also exhibit less sintering distortion. A set of parameters was investigated to alter and sufficiently influence shrinkage during sintering to obtain parts to print. In addition, a new tool that incorporates directional shrink factors as determined for compound B was designed and obtained at the end of this reporting period.

The following highlights relate to activities carried out on parts molded in the old tool.

- Previously molded and baked stator segments made with composition modifications B-2 and B-3, whereby B-2 has a higher plastic content than B-3, were sintered at temperatures lower than standard.

- A matrix approach was used in determining the sintering temperature that would yield the best dimensions in connection with an acceptable final density for each of these mix modifications.

- Stator segments made with B-3 compound that were sintered at the lowest matrix temperature gave the best overall dimensional results. Correspondingly made MOR bars were processed using the same sintering parameters.

- Thirty stator segments of composition B-2 and 100 of B-3 were sintered at the newly established conditions.

- Forty-six B-3 stator segments (2 sets) passed all the required inspection steps but were still slightly under size. The parts were sent to Garrett for evaluation.

- Standard mix was used for molding 250 stator segments. All parts were processed using standard procedures and conditions. Some of these parts were used to determine mold dimensions for a new injection molding tool.

- The remaining parts were used for fixturing experiments during sintering. Warpage of the sidewalls, flaring at the ends and some distortion in the trailing edge necessitated additional design work on the sintering fixtures. A configuration was developed that was successful in eliminating these deviations.

- Forty new sintering fixtures were obtained.

- Standard compound has been prepared for use in the new injection molding tools that had been received at the end of the reporting period.

3.2 Turbine Shroud

The turbine shroud, at about 15 pounds is the largest injection molded SASC part processed by Carborundum and is made on a 1000-ton injection molding machine at a customer molder. Work on the newly designed turbine shroud, Drawing PA3609679, was resumed during the second half of this reporting period.

- The old injection molding tooling was redesigned and modified in areas with sufficient stock to accommodate the new requirements. However, additional green machining of the as-molded parts will be necessary to obtain all aspects of the new design. Additional grinding stock in the flange area was incorporated to allow for some distortion during sintering.

- Two different mixes (B and D) were compounded.

- An injection molding run was scheduled for December 1983 and yielded 19 turbine shrouds of mix B and 20 of mix D for further processing.

- All parts show some flow lines. Most of the flow lines, however, are in areas where stock will be removed during green machining (Figure 49)

- Four shrouds were green machined in the as-molded state (Figure 50) and will be submitted for initial NDE inspection.

3.3 Combustor Baffle

The combustor baffle has been fabricated by slip casting using a bimodal water based SiC composition. The drain casting method used yields a reproducible outside configuration but additional green machining of the inside contour is necessary to obtain the desired profile with constant wall thickness.

An advanced plastic forming method has been chosen to replace slip casting as a forming process. The new method is expected to produce combustor baffles near net shape,

Figure 49. As-Molded Turbine Shroud.

Figure 50. Green Machined Turbine Shroud.

eliminating all green machining work. An attempt is made to closely duplicate the bimodal ratio of the SiC powder of the casting slurry to obtain a comparable final density.

Paragraphs 3.3.1 and 3.3.2 summarize the activities on combustor baffles carried out on both forming methods:

3.3.1 Combustor Baffle (Cast)

- Fifty combustor baffles were cast before work in this area was halted. The parts subsequently were processed through air drying and high temperature bake.
- Thirty parts were green machined on the inside contour and cleaned prior to sintering.
- Seven completely processed combustor baffles passed as-fired NDE inspection and were shipped to Garrett with corresponding MOR bars.
- One combustor baffle remains as work-in-process in NDE.

3.3.2 Combustor Baffle (Plastic Forming)

- Initial trials were conducted on two bimodal plastic compounds (P-1 and P-2) which varied in the plastic content with compound P-2 having less plastics than P-1.
- Both compounds showed good molding characteristics but compound P-2 was less susceptible to bake-out problems and was therefore chosen for further forming trials.
- Flat disks of 1/2 to 1 inch thickness were formed using different molding pressures and temperatures. These disks were used for initial shrinkage, density, and strength determinations.
- The steel tool for the combustor baffle was received and first trials showed good surface quality on the as-molded parts, but cracking on the ID and partially unfilled locating tabs necessitated revisions of the mold and the insert.
- The problem of proper flow and filling characteristics to obtain a homogeneously

dense body with good surface quality was addressed by evaluating different methods of charging the mold.

- New molding trials are scheduled for early January 1984.

3.4 Transition Duct

This part has been made by isopressing a tube billet and green machining the inside and outside contour using a CNC lathe. Each part is sintered on a contoured mandrel and only minor grinding work is required on the ends and the inside platform (transition duct/combustor baffle interface).

- Six tube billets were isopressed.
- Two of these parts were made using submicron SiC powder having a modified particle size distribution.
- Parts from the previous as well as current reporting period have been identically processed according to standard procedures.
- Four machined transition ducts corresponding basically to drawing 3846232 were completed and shipped with corresponding MOR bars to Garrett. Slight design modifications are being incorporated per request as soon as feasible. All of the shipped parts had additional stock on the platform and the last transition duct also incorporated additional stock in length (transition duct/turbine shroud interface).
- Three transition ducts were green machined, passed green inspection, and will be sintered in early January 1984.

3.5 Combustor Liner

Plastic extrusion has been chosen to replace isopressing/green machining as the forming process for combustor liners. This part is ideally suited for this new processing technique, which has a high volume potential. Current activities are focused on scale up with respect to extrusion and processing of large diameter tubing.

- Standard extrusion mix was compounded; no mix variations were undertaken.
- All parts were extruded at a custom molding facility. Extrusion experiments with respect to temperature distributions and extrusion speed were conducted. Modifications of take-up equipment were necessary for minimizing deformation and adequately controlling cool-down.
- Initially extruded parts were oversized on the OD, showed surface imperfections and internal defects.
- Additional stock was subsequently incorporated by enlarging the extrusion die. The distribution of the extrusion temperatures was changed, eliminating most of the visually detectable surface flaws.
- A new extrusion run was conducted late during this reporting period yielding tube stock for about 26 individual liners.
- Various bake-out and sintering techniques were investigated and a set of new procedures was established.
- Two parts progressed through bake-out and sintering and are currently in grinding.

3.6 Regenerator Shield

Previously supplied parts were made by isopressing/green machining and final grinding. Again plastic extrusion was chosen as an advanced forming process for this component minimizing powder requirements and eliminating green machining costs.

- The first extrusion trial was unsuccessful because of insufficient filling pressure supplied by the extruder originally chosen.
- Scale-up problems were encountered and dies for a larger extruder and specific take-up equipment for this extruder had to

be designed. The green extruded tube has roughly a diameter of 7 and 3/4 inches, a considerable step up from the combustor liner which has about a 5-inch diameter.

- Because of the delay in obtaining adequate forming equipment and the need for delivering ground parts to Garrett two isopressed/green machined parts were initiated in September 1983.

- Both isopressed/green machined parts were processed through sintering and as-fired NDE. One of these parts remains in grinding; the other was ground, passed final QC and was shipped to Garrett with corresponding MOR bars.

- Two additional isopressed billets were prepared in December 1983, green machined and sintered.

- The parts passed as-fired QC and were submitted for final grinding.

- The second extrusion run, using a larger extruder produced tube stock, which yields about 26 individual regenerator shields.

- Four extruded regenerator shields were cut to size, inspected, and submitted for binder removal.

- One of these parts completed bake-out, was sintered and submitted for as-fired QC.

- All work-in-process, isopressed/green machined and extruded, will be processed parallel to meet delivery requirements.

APPENDIX D

LIST OF SYMBOLS, ABBREVIATIONS AND ACRONYMS

Acronyms	Definition
ACC	AiResearch Casting Company
AGT	advanced gas turbine
AGT101	the AGT model being developed by Garrett/Ford
Al_2O_3	aluminum oxide
AS	aluminum silicate
BN	Borazon
^oC	degrees Celsius
CBO	The Carborundum Company
C_L	clearance probes
CFDC	Combined Federal Driving Cycle
CNC	computer numerical control
CO	carbon monoxide
CO_2	carbon dioxide
DAW	dual alloy wheel
DFC	diffusion flame combustor
DOE	U.S. Department of Energy
DS	directionally solidifed
ECU	electronic control unit
EDX	energy dispersive X-ray
EPA	Environmental Protection Agency
^oF	degrees Fahrenheit
Ford 707	an industrial gas turbine engine by Ford
FY	fiscal year
GE	General Electric Company
HC	hydrocarbon
HCl	hydrogen chloride
Hexoloy^{TM} KX01	Carborundum material, SiC
Hexoloy^{TM} KX02	Carborundum material, SiC
Hexoloy^{TM} SA	Carborundum material, SiC
Hf	halfnium
HIP	hot isostatic pressing
HP	high pressure regenerator inlet (cold side)
HTP	high temperature protection, Lockheed
Hz	Hertz (frequency)
ID	inner diameter
IGV	inlet guide vane (compressor)
IR&D	internal research and development
I-112	regenerator seal coating material
JP-4	jet propulsion fuel Number 4
ksi	thousand pounds per square inch
lb/min	pounds per minute
lb-ft	pound feet (of torque)
LBO	lean blowout

LIST OF SYMBOLS, ABBREVIATIONS AND ACRONYMS (Contd)

Acronyms	Definition
LCF	low cycle fatigue
LDV	laser Doppler velocimeter
LP	low pressure regenerator inlet (hot side)
"m"	Weibull modulus
MAS	magnesium aluminum silicate
MEK	methyl ethyl ketone
MENTOR II	Ford regenerator computer program
METCO 443	flame spray coating
METCO 447	flame spray coating
MgO	magnesium oxide
Mod I	first development engine
Mod II	second generation ceramic engine
MOR	modulus of rupture
N	rotational speed
N_{ps}	population, number of samples
NASA	National Aeronautics and Space Administration
NGK	NGK-Locke, Inc.
NiCr	nickel chrome alloy
NO_x	oxides of nitrogen
OD	outer diameter
PM	powder metal
PN	part number
LB/MIN	pounds per minute
LB/HR	pounds per hour
PR_C	compressor pressure ratio
P_S	static pressure
PR_T	turbine pressure ratio
psia	pounds pressure per square inch, absolute
psid	pounds pressure per square inch, differential
psig	pounds pressure per square inch, gauge
P_T	total pressure
PWM	pulse width modulated
RBN 104	ACC RBSN material
RBN 124	ACC RBSN material
RBSiC	reaction bonded silicon carbide
RBSN	reaction bonded silicon nitride
RCG	reaction cured glass, Lockheed
RM-1	Ford rotor material, first generation
RM-2	Ford rotor material, second generation
RM-3	Ford rotor material, third generation
RMS	root mean square
RPD	reference powertrain design
rpm	revolutions per minute
RSSiC	reaction sintered silicon carbide
SASC	Carborundum material, Hexoloy™, α-SiC
SEM	scanning electron microscopy

LIST OF SYMBOLS, ABBREVIATIONS AND ACRONYMS (Contd)

Acronyms	Definition
SiC	silicon carbide
Si_3N_4	silicon nitride
SMD	sauter mean diameter
S/N	serial number
SNN 522	ACC sintered silicon nitride
SN-50	NGK silicon nitride material
SR	stress rupture
SRBSN	sintered RBSN
TC	thermocouple
TD	theoretical density
TIR	total indicator reading
TIT	turbine inlet temperature
TRW	Thompson Ramo Woldridge
T_T	total temperature
T-T	total-to-total
VIGV	variable inlet guide vane
W_t	speed
W	tungsten
W-K	Wayne-Kerr
yo-yo	Astroloy heat treat cycle
Y_2O_3	yttrium oxide
β	beta
$\Delta T/T$	delta temperature/temperature standard
μ	micro strain
$\Delta P/P$	delta pressure/pressure standard
A	characteristic strength

REFERENCES

1) Garrett Turbine Engine Company, "Advanced Gas Turbine (AGT) Powertrain System Development for Automotive Applications", Semiannual Progress Report Number 1 (October 1979 through June 1980), NASA Report CR- 165175, November 1980, Contract DEN3-167.

2) Garrett Turbine Engine Company, "Advanced Gas Turbine (AGT) Powertrain System Development for Automotive Applications", Semiannual Progress Report Number 2. (July 1980 through December 1980), NASA Report CR-165329, June 1981, Contract DEN3-167.

3) Garrett Turbine Engine Company, "Advanced Gas Turbine (AGT) Powertrain System Development for Automotive Applications", Semiannual Progress Report Number 3 (January 1981 through June 1981), NASA Report CR- 167901, December 1981, Contract DEN3-167.

4) Garrett Turbine Engine Company, "Advanced Gas Turbine (AGT) Powertrain System Development for Automotive Applications", Semiannual Progress Report Number 4. (July 1981 through December (1981), NASA Report CR-167983, June 1982, Contract DEN3-167.

5) Garrett Turbine Engine Company, "Advanced Gas Turbine (AGT) Powertrain System Development for Automotive Applications," Semiannual Progress Report Number 5. (January 1982 through June 1982), NASA Report CR-168104, December 1982, Contract DEN3-167.

6) Garrett Turbine Engine Company, "Advanced Gas Turbine (AGT) Powertrain System Development for Automotive Applications," Semiannual Progress Report Number 6. (July 1982 through December 1982), NASA Report CR-168246 June 1983, Contract DEN3-167.

7) Garrett Turbine Engine Company, "Advanced Gas Turbine (AGT) Powertrain System Development for Automotive Applications", Semiannual Progress Report Number 7. (January 1983 through June 1983), NASA Report CR-174694 December 1983, Contract DEN3-167.